

Inferences and Implications for  
Parameterizations from a  
Global Diagnosis of Mesoscale Tracer Stirring

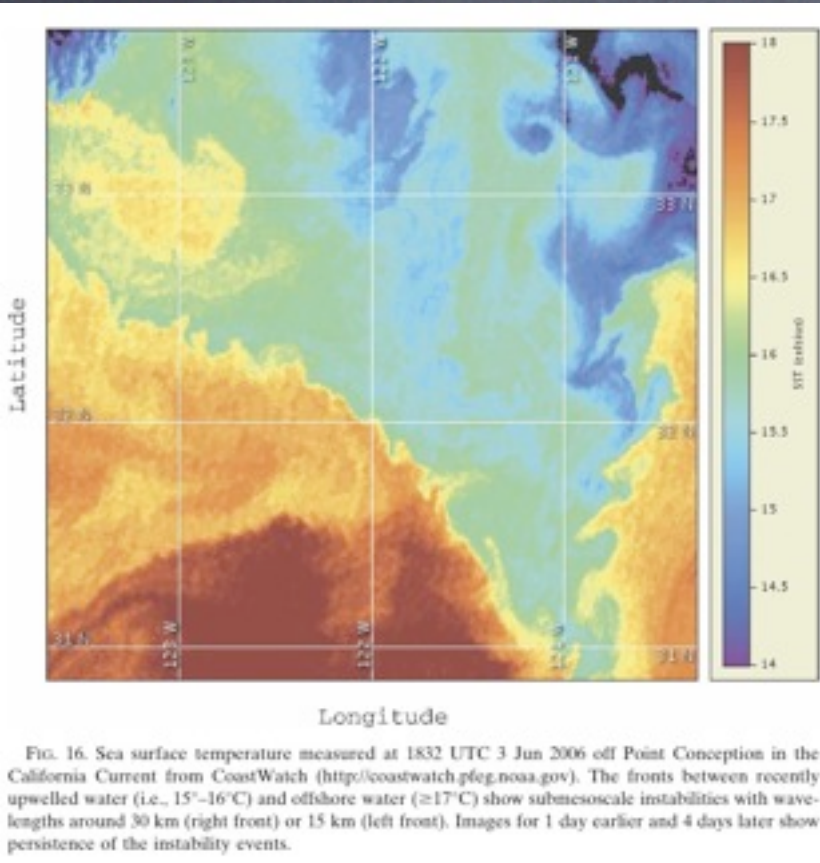
Baylor Fox-Kemper,  
with Frank Bryan, John Dennis,  
Andrew Margolin, and Scott Bachman

OMWG Meeting, 12/11 9:25–9:45

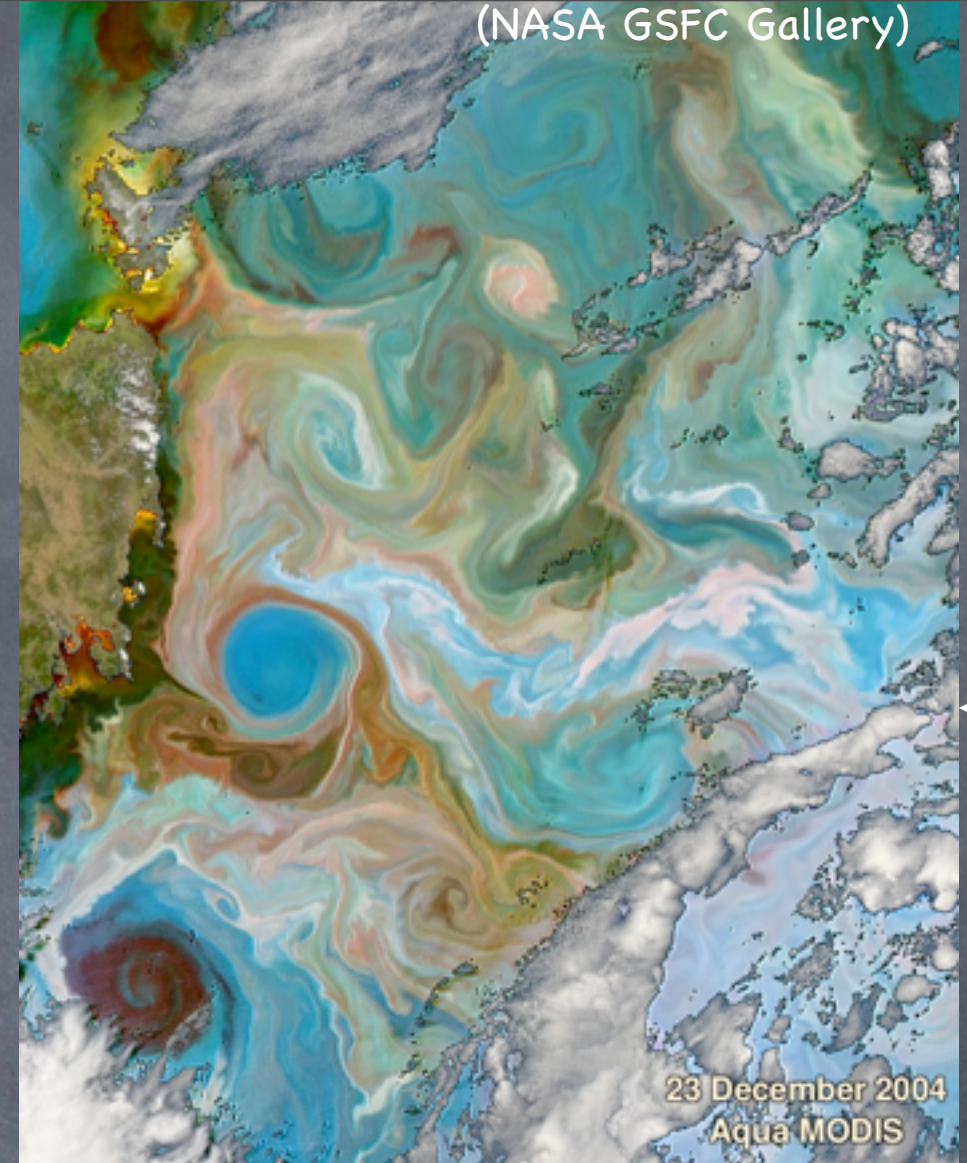


# The Character of the Mesoscale

(Capet et al., 2008)



- Boundary Currents
- Eddies
- $Ro=O(0.1)$
- $Ri=O(1000)$
- Full Depth
- Projects on Fronts
- 100km, months



Eddy processes mainly **baroclinic & barotropic instability**.  
Parameterizations of baroclinic instability (GM, Visbeck...).



# Tracer Flux-Gradient Relationship

$$\overline{\mathbf{u}'\tau'} = -\mathbf{M}\nabla\bar{\tau}$$

- Virtually all extant subgridscale eddy closures may be written as above, e.g.: GM, Redi, FFH
- Relates the eddy flux to the coarse-grain gradients
- May have a flow/property dependent  $\mathbf{M}$ :  
(FFH, Visbeck, Green, Held & Larichev, Stone, Canuto & Dubovikov, Griffies et al '05)
- May consider gridscale (FFH, Hallberg & Adcroft)
- Isopycnal & lagrangian coordinate versions possible/known



$$\overline{\mathbf{u}'\tau'} = -\mathbf{M}\nabla\bar{\tau}$$

## General Form

$$\begin{bmatrix} \overline{u'\tau'} \\ \overline{v'\tau'} \\ \overline{w'\tau'} \end{bmatrix} = - \begin{bmatrix} M_{xx} & M_{xy} & M_{xz} \\ M_{yx} & M_{yy} & M_{yz} \\ M_{zx} & M_{zy} & M_{zz} \end{bmatrix} \begin{bmatrix} \bar{\tau}_x \\ \bar{\tau}_y \\ \bar{\tau}_z \end{bmatrix}$$

- Diagnostically: 9 elements requires at least 3 similar-transport tracers to specify uniquely
- Could vary tracer by tracer, or active tracer vs. passive, etc. In practice we don't do this.



$$\overline{\mathbf{u}'\tau'} = -\mathbf{M}\nabla\bar{\tau}$$

## Anisotropic\* Redi Form

$$\begin{bmatrix} \overline{u'\tau'} \\ \overline{v'\tau'} \\ \overline{w'\tau'} \end{bmatrix} = - \begin{bmatrix} K_{xx} & K_{xy} & \hat{x}\cdot\mathbf{K}\cdot\tilde{\nabla}_z \\ K_{yx} & K_{yy} & \hat{y}\cdot\mathbf{K}\cdot\tilde{\nabla}_z \\ \hat{x}\cdot\mathbf{K}\cdot\tilde{\nabla}_z & \hat{y}\cdot\mathbf{K}\cdot\tilde{\nabla}_z & \tilde{\nabla}_z\cdot\mathbf{K}\cdot\tilde{\nabla}_z \end{bmatrix} \begin{bmatrix} \bar{\tau}_x \\ \bar{\tau}_y \\ \bar{\tau}_z \end{bmatrix}$$

**Yellow** Elements are horizontal stirring

**Blue** Elements in Redi (1982) are **symmetric**  
and scaled to make

**eddy mixing along neutral surfaces**

\*Anisotropic form due to Smith & Gent 04



$$\overline{\mathbf{u}'\tau'} = -\mathbf{M}\nabla\bar{\tau}$$

## Anisotropic\* Gent-McWilliams

$$\begin{bmatrix} \overline{u'\tau'} \\ \overline{v'\tau'} \\ \overline{w'\tau'} \end{bmatrix} = - \begin{bmatrix} 0 & 0 & -\hat{x}\cdot\mathbf{K}\cdot\tilde{\nabla}_z \\ 0 & 0 & -\hat{y}\cdot\mathbf{K}\cdot\tilde{\nabla}_z \\ \hat{x}\cdot\mathbf{K}\cdot\tilde{\nabla}_z & \hat{y}\cdot\mathbf{K}\cdot\tilde{\nabla}_z & 0 \end{bmatrix} \begin{bmatrix} \bar{\tau}_x \\ \bar{\tau}_y \\ \bar{\tau}_z \end{bmatrix}$$

Antisymmetric Elements in GM (1990)

are scaled to overturn fronts, make vertical fluxes extract PE, and restratify the fluid equivalent to eddy-induced advection

Q: Same K as Redi?

\*Anisotropic form due to Smith & Gent 04 \*Tensor Form (Griffies, 98)



$$\overline{\mathbf{u}'\tau'} = -M\nabla\bar{\tau}$$

Fox-Kemper, Ferrari, & Hallberg (2008) form  
(a mixed layer (submeso) eddy param.):

$$\begin{bmatrix} \overline{u'\tau'} \\ \overline{v'\tau'} \\ \overline{w'\tau'} \end{bmatrix} = - \begin{bmatrix} 0 & 0 & -\Psi_y \\ 0 & 0 & \Psi_x \\ \Psi_y & -\Psi_x & 0 \end{bmatrix} \begin{bmatrix} \bar{\tau}_x \\ \bar{\tau}_y \\ \bar{\tau}_z \end{bmatrix}$$

**Antisymmetric** Elements in Fox-Kemper, Ferrari, & Hallberg (2008) are scaled to **overtake fronts**, make vertical fluxes **extract PE**, and **restratify the fluid**,  
At a rate validated against eddying simulations!



# Need a Natural, Mesoscale Eddy Environment to Test Out:

$$\overline{\mathbf{u}'\tau'} = -\mathbf{M}\nabla\bar{\tau}$$

$$\begin{bmatrix} \overline{u'\tau'} \\ \overline{v'\tau'} \\ \overline{w'\tau'} \end{bmatrix} = - \begin{bmatrix} M_{xx} & M_{xy} & M_{xz} \\ M_{yx} & M_{yy} & M_{yz} \\ M_{zx} & M_{zy} & M_{zz} \end{bmatrix} \begin{bmatrix} \bar{\tau}_x \\ \bar{\tau}_y \\ \bar{\tau}_z \end{bmatrix}$$

3 equations/tracer

9 unknowns (**M** components)

BY USING 3 or MORE TRACERS, can determine **M**!!!

(a la Plumb & Mahlman '87, Bratseth '98)



Use a Natural, Mesoscale Eddy  
Environment to Test Out:

$$\overline{\mathbf{u}'\tau'} = -M\nabla\bar{\tau}$$

We Use:

Years 16–20 of a Global 0.1 Degree  
Model (sim to Maltrud & McClean '06)

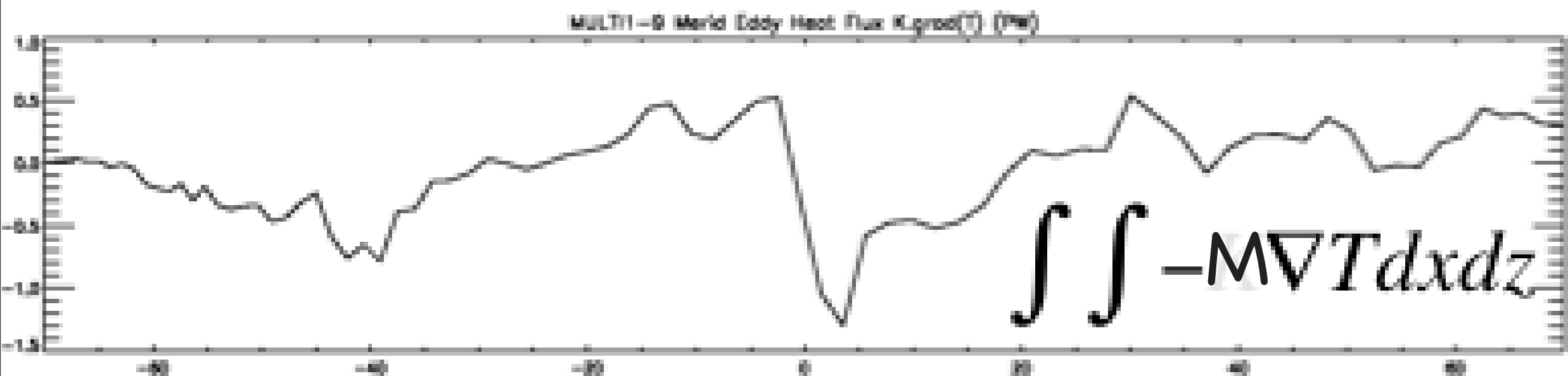
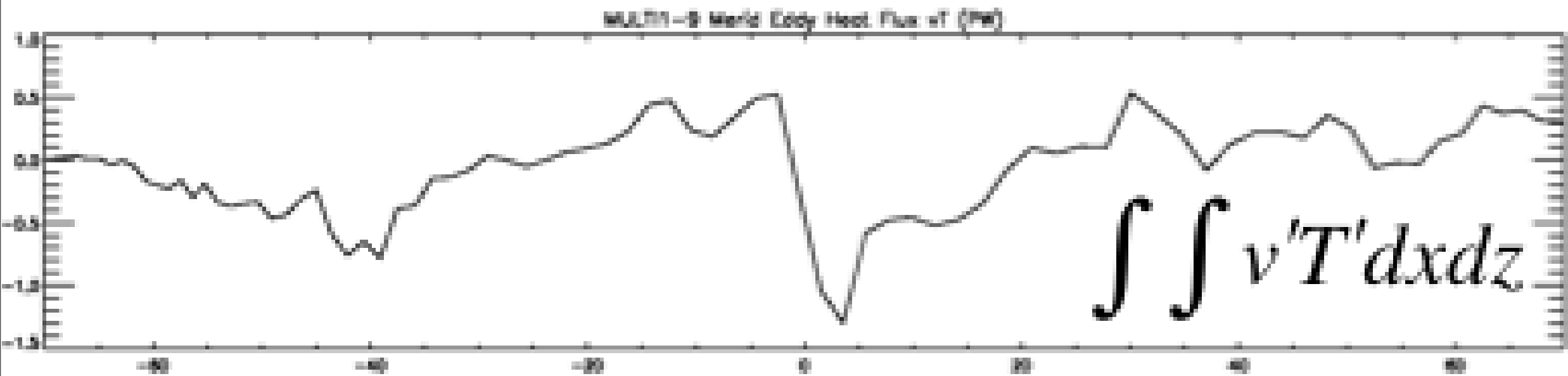
9 Passive Tracers To Overdetermine  $M$



# Use a Natural, Mesoscale Eddy Environment to Test Out:

## Testing the Diagnosis:

Note: T not used for diagnosis, active tracers are apparently transported as passive ones are!



Differences: Diffusion - Eddy

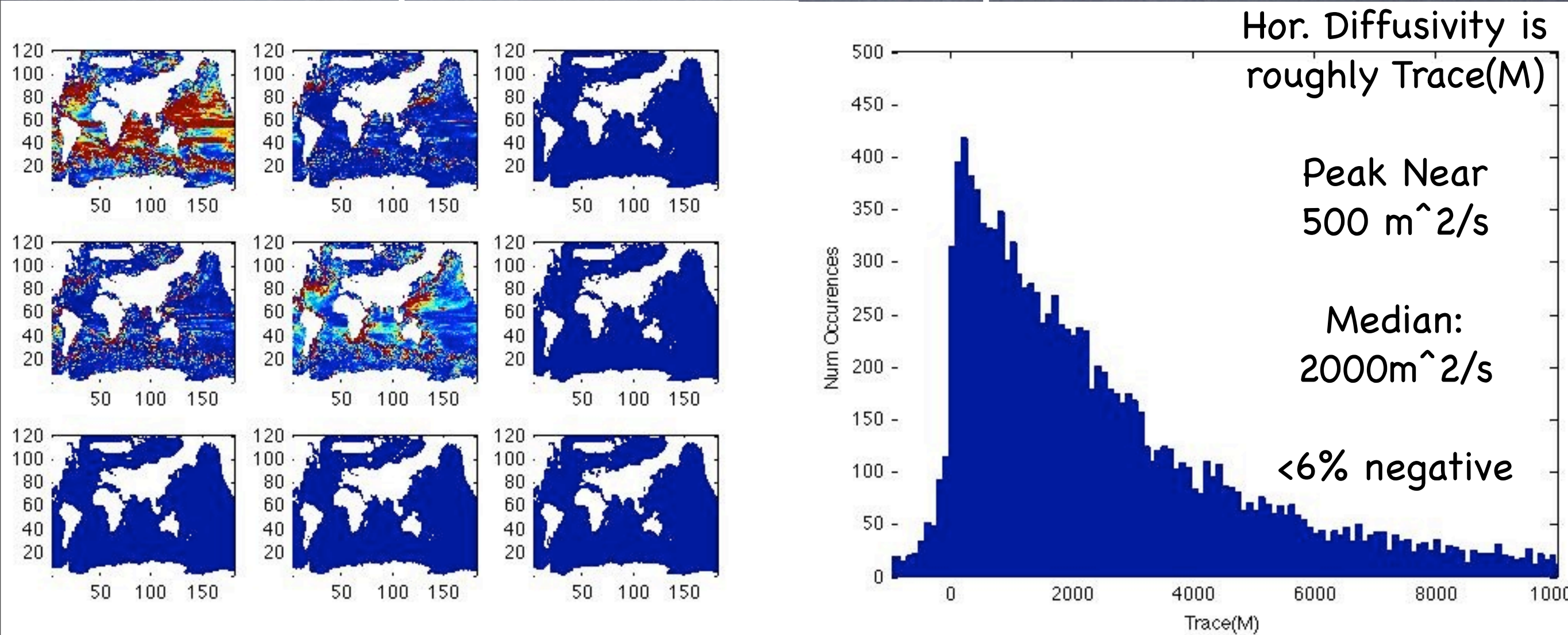


# Use a Natural, Mesoscale Eddy

Environment to Test Out:

$$\begin{bmatrix} \overline{u'\tau'} \\ \overline{v'\tau'} \\ \overline{w'\tau'} \end{bmatrix} = - \begin{bmatrix} K_{xx} & K_{xy} & \hat{x} \cdot \mathbf{K} \cdot \tilde{\nabla} \mathbf{z} \\ K_{yx} & K_{yy} & \hat{y} \cdot \mathbf{K} \cdot \tilde{\nabla} \mathbf{z} \\ \hat{x} \cdot \mathbf{K} \cdot \tilde{\nabla} \mathbf{z} & \hat{y} \cdot \mathbf{K} \cdot \tilde{\nabla} \mathbf{z} & \tilde{\nabla} \mathbf{z} \cdot \mathbf{K} \cdot \tilde{\nabla} \mathbf{z} \end{bmatrix} \begin{bmatrix} \overline{\tau}_x \\ \overline{\tau}_y \\ \overline{\tau}_z \end{bmatrix}$$

Correct shape/scale at 150m depth:





# Use a Natural, Mesoscale Eddy

Environment to Test Out:

$$\begin{bmatrix} \overline{u'\tau'} \\ \overline{v'\tau'} \\ \overline{w'\tau'} \end{bmatrix} = - \begin{bmatrix} 0 & 0 & -\hat{x} \cdot \mathbf{K} \cdot \tilde{\nabla}_z \\ 0 & 0 & -\hat{y} \cdot \mathbf{K} \cdot \tilde{\nabla}_z \\ \hat{x} \cdot \mathbf{K} \cdot \tilde{\nabla}_z & \hat{y} \cdot \mathbf{K} \cdot \tilde{\nabla}_z & 0 \end{bmatrix} \begin{bmatrix} \overline{\tau}_x \\ \overline{\tau}_y \\ \overline{\tau}_z \end{bmatrix}$$

Result 1: Antisymmetric (GM) Elements  
scale with  
corresponding Symmetric (Redi)  
elements in extratropics.

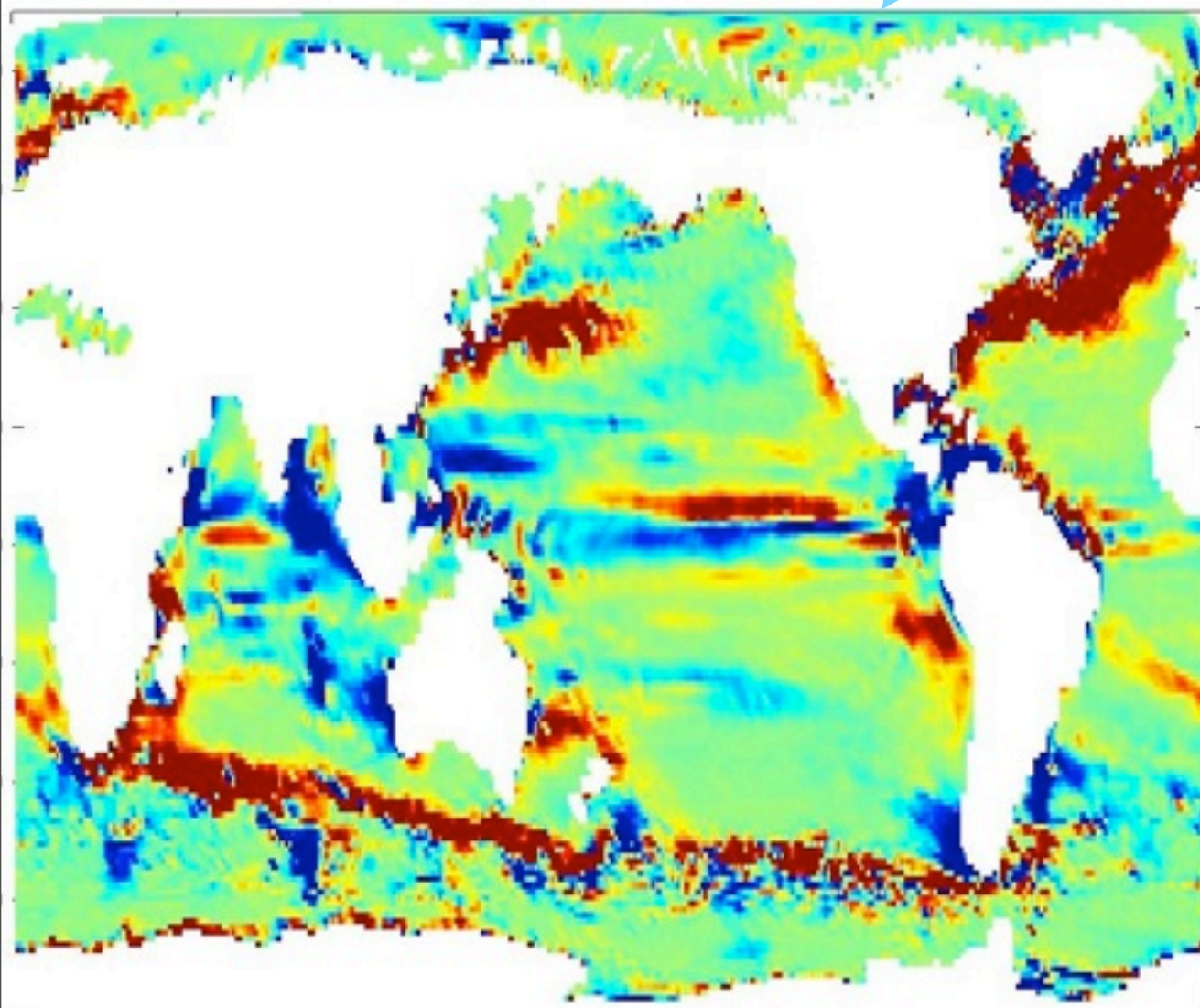
Thus, GM/Redi basic shape of M is  
roughly correct  
(some detailed validation remains)



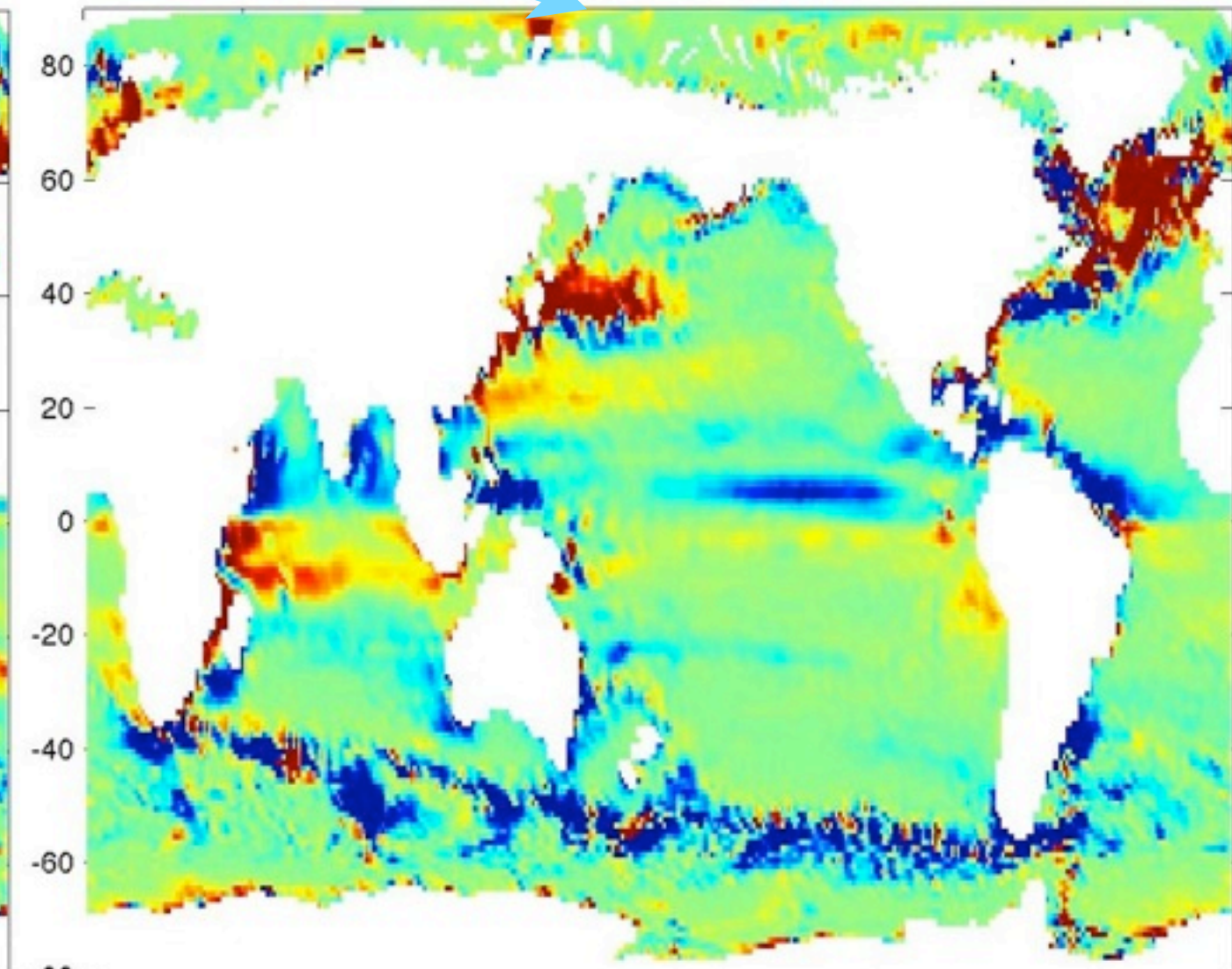
# Use a Natural, Mesoscale Eddy Environment to Test Out:

$$\begin{bmatrix} \overline{u'\tau'} \\ \overline{v'\tau'} \\ \overline{w'\tau'} \end{bmatrix} = - \begin{bmatrix} 0 & 0 & -\hat{x} \cdot \mathbf{K} \cdot \tilde{\nabla} \mathbf{z} \\ 0 & 0 & -\hat{y} \cdot \mathbf{K} \cdot \tilde{\nabla} \mathbf{z} \\ \hat{x} \cdot \mathbf{K} \cdot \tilde{\nabla} \mathbf{z} & \hat{y} \cdot \mathbf{K} \cdot \tilde{\nabla} \mathbf{z} & 0 \end{bmatrix} \begin{bmatrix} \overline{\tau}_x \\ \overline{\tau}_y \\ \overline{\tau}_z \end{bmatrix}$$

Asym 3,1: GM@z=-149rr



Asym 3,2: GM@z=-149rr

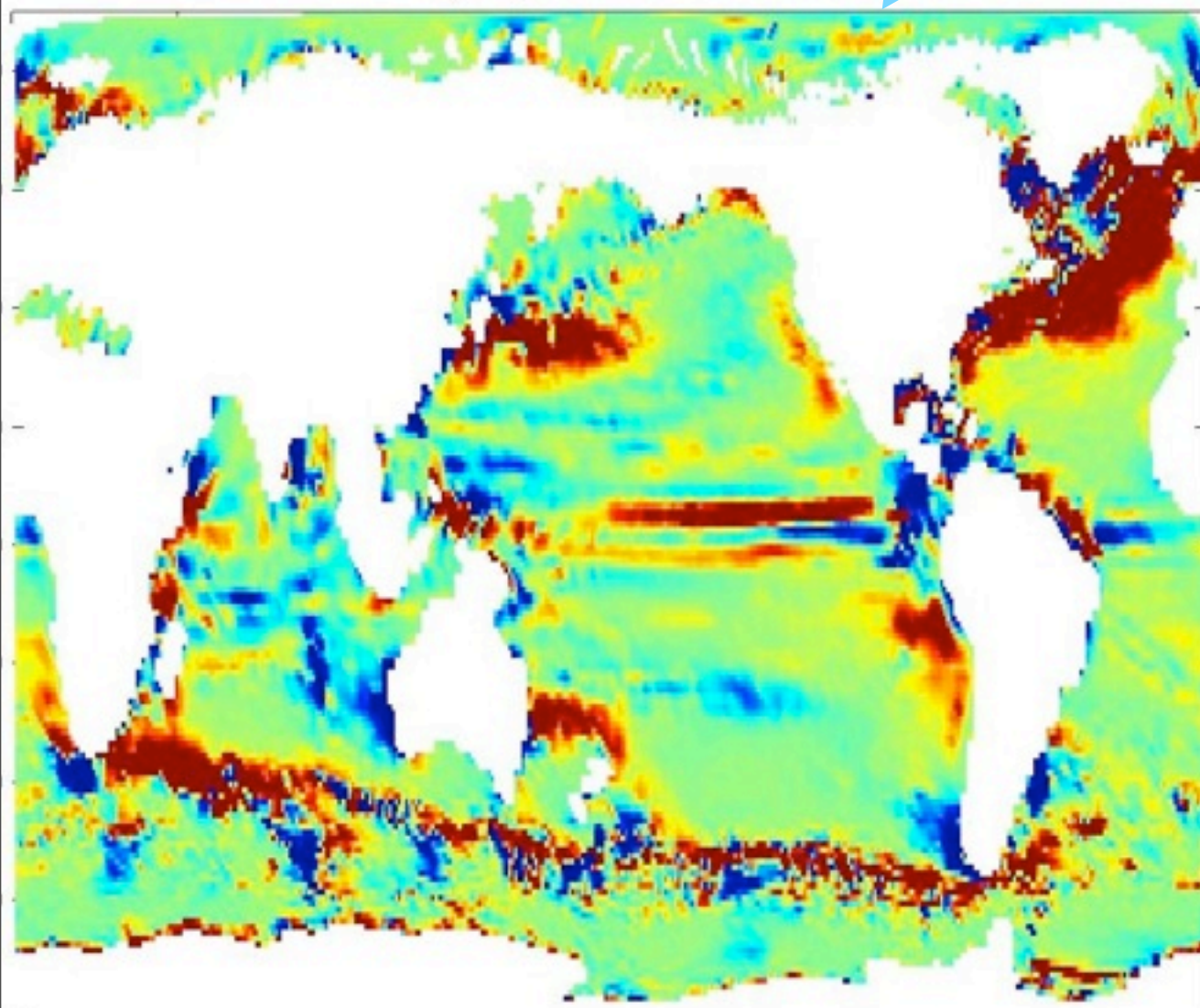




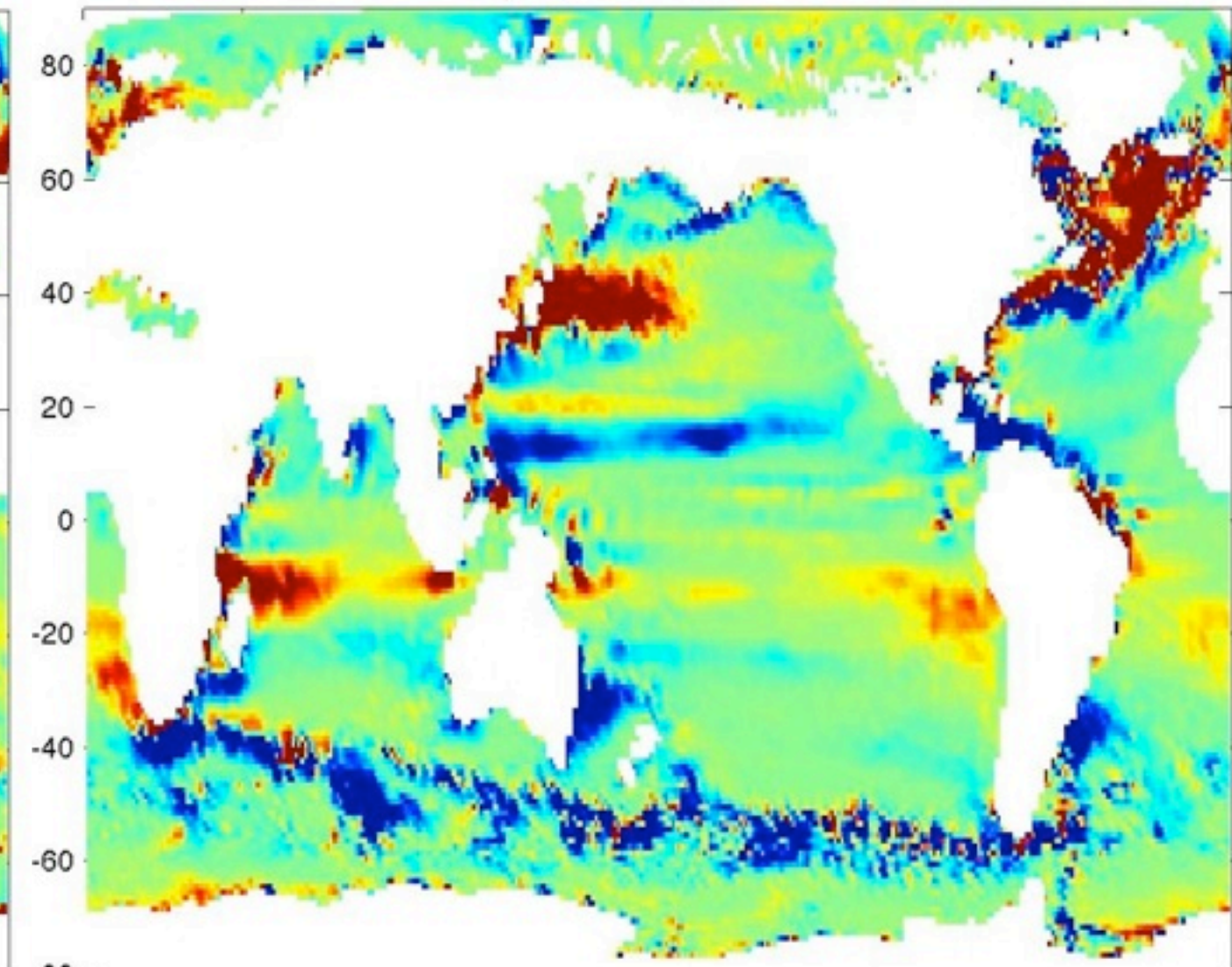
# Use a Natural, Mesoscale Eddy Environment to Test Out:

$$\begin{bmatrix} \overline{u'\tau'} \\ \overline{v'\tau'} \\ \overline{w'\tau'} \end{bmatrix} = - \begin{bmatrix} K_{xx} & K_{xy} & \hat{x} \cdot \mathbf{K} \cdot \tilde{\nabla} \mathbf{z} \\ K_{yx} & K_{yy} & \hat{y} \cdot \mathbf{K} \cdot \tilde{\nabla} \mathbf{z} \\ \hat{x} \cdot \mathbf{K} \cdot \tilde{\nabla} \mathbf{z} & \hat{y} \cdot \mathbf{K} \cdot \tilde{\nabla} \mathbf{z} & \tilde{\nabla} \mathbf{z} \cdot \mathbf{K} \cdot \tilde{\nabla} \mathbf{z} \end{bmatrix} \begin{bmatrix} \overline{\tau}_x \\ \overline{\tau}_y \\ \overline{\tau}_z \end{bmatrix}$$

Sym 3,1: Redi@z=-149m



Sym 3,2: Redi@z=-149m



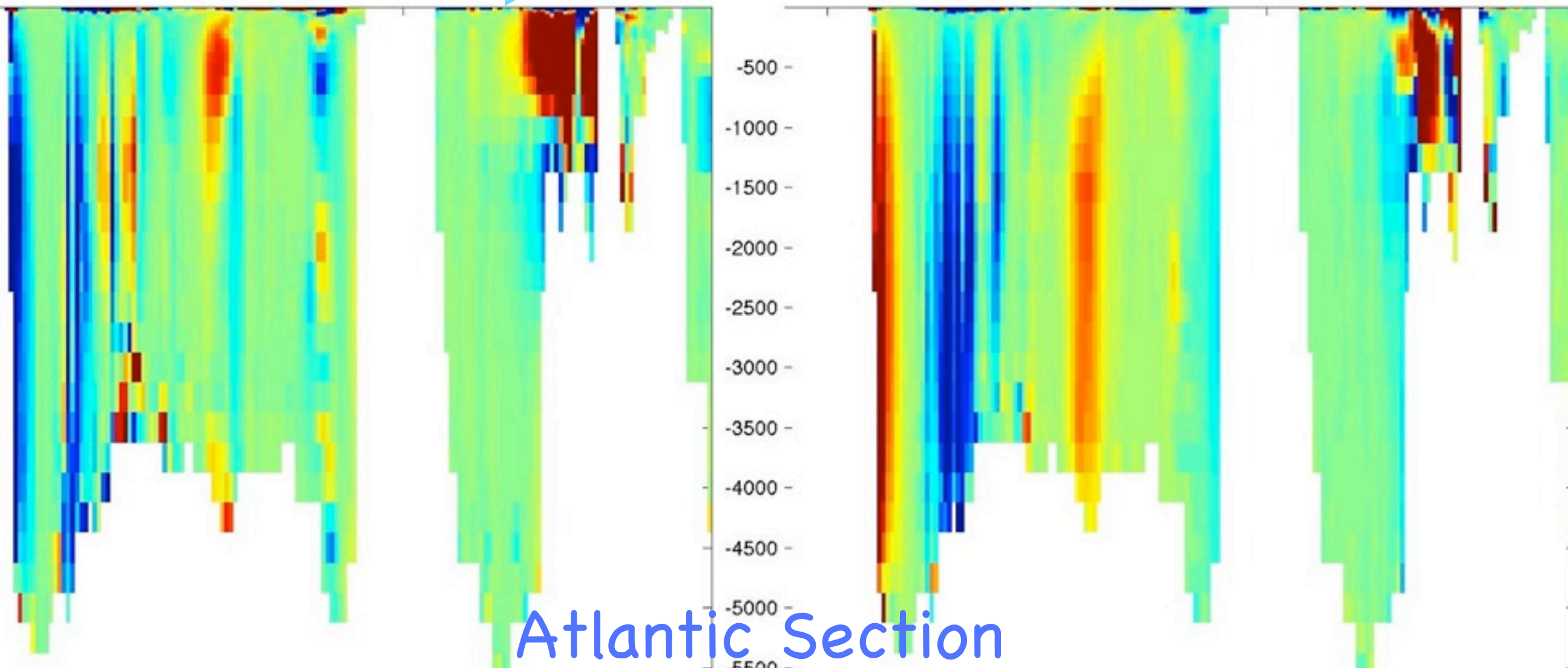


# Use a Natural, Mesoscale Eddy Environment to Test Out:

$$\begin{bmatrix} \overline{u'\tau'} \\ \overline{v'\tau'} \\ \overline{w'\tau'} \end{bmatrix} = - \begin{bmatrix} 0 & 0 & -\hat{x} \cdot \mathbf{K} \cdot \tilde{\nabla} \mathbf{z} \\ 0 & 0 & -\hat{y} \cdot \mathbf{K} \cdot \tilde{\nabla} \mathbf{z} \\ \hat{x} \cdot \mathbf{K} \cdot \tilde{\nabla} \mathbf{z} & \hat{y} \cdot \mathbf{K} \cdot \tilde{\nabla} \mathbf{z} & 0 \end{bmatrix} \begin{bmatrix} \overline{\tau}_x \\ \overline{\tau}_y \\ \overline{\tau}_z \end{bmatrix}$$

Asym 3,1: GM@lon=345E

Asym 3,2: GM@lon=345E



Atlantic Section

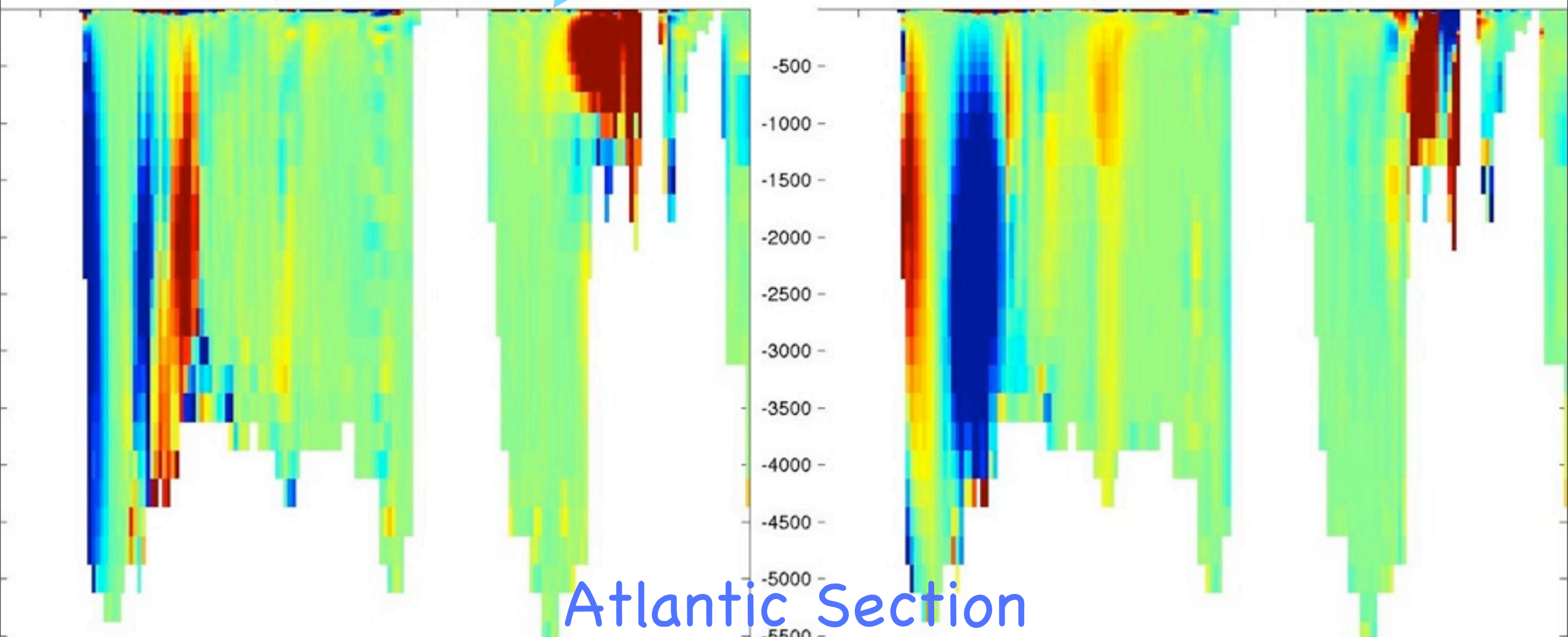


# Use a Natural, Mesoscale Eddy Environment to Test Out:

$$\begin{bmatrix} \overline{u'\tau'} \\ \overline{v'\tau'} \\ \overline{w'\tau'} \end{bmatrix} = - \begin{bmatrix} K_{xx} & K_{xy} & \hat{x} \cdot \mathbf{K} \cdot \tilde{\nabla} \mathbf{z} \\ K_{yx} & K_{yy} & \hat{y} \cdot \mathbf{K} \cdot \tilde{\nabla} \mathbf{z} \\ \hat{x} \cdot \mathbf{K} \cdot \tilde{\nabla} \mathbf{z} & \hat{y} \cdot \mathbf{K} \cdot \tilde{\nabla} \mathbf{z} & \tilde{\nabla} \mathbf{z} \cdot \mathbf{K} \cdot \tilde{\nabla} \mathbf{z} \end{bmatrix} \begin{bmatrix} \overline{\tau}_x \\ \overline{\tau}_y \\ \overline{\tau}_z \end{bmatrix}$$

Sym 3,1: Redi@lon=345E

Sym 3,2: Redi@lon=345E



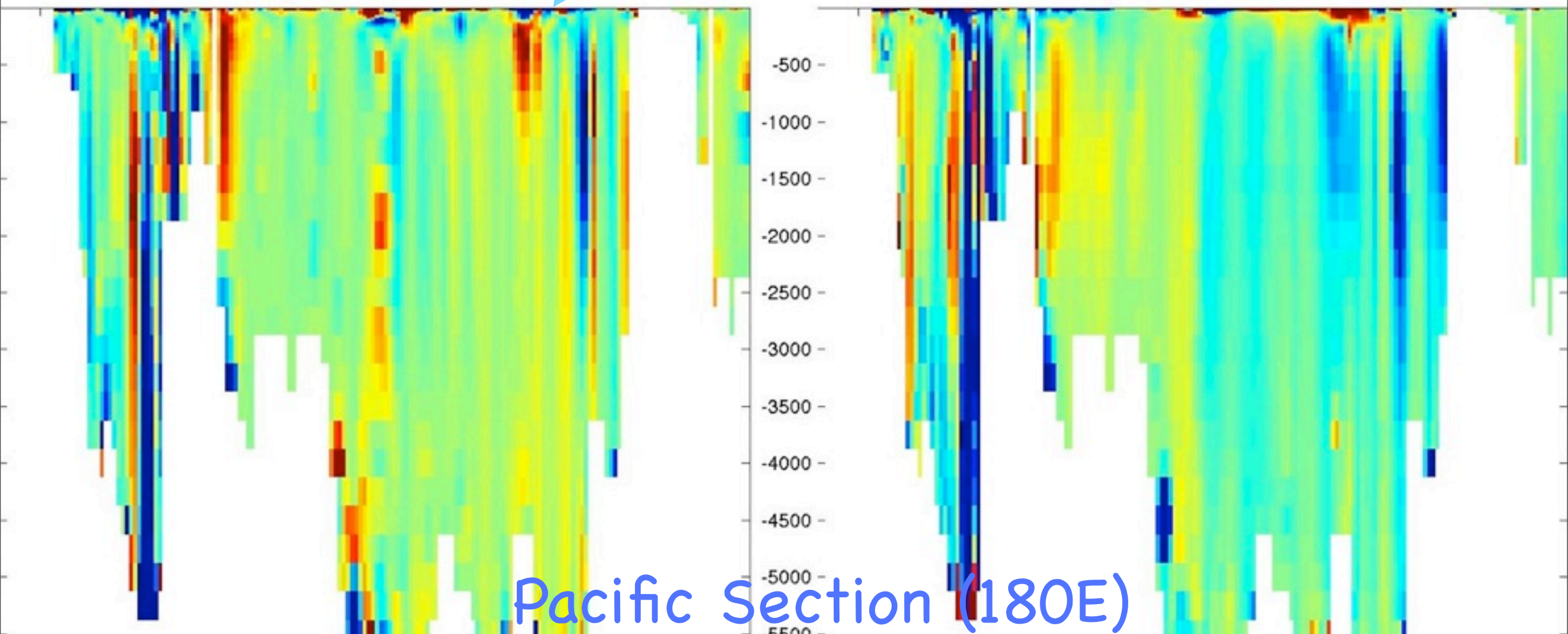


# Use a Natural, Mesoscale Eddy Environment to Test Out:

$$\begin{bmatrix} \overline{u'\tau'} \\ \overline{v'\tau'} \\ \overline{w'\tau'} \end{bmatrix} = - \begin{bmatrix} 0 & 0 & -\hat{x} \cdot \mathbf{K} \cdot \tilde{\nabla}_z \\ 0 & 0 & -\hat{y} \cdot \mathbf{K} \cdot \tilde{\nabla}_z \\ \hat{x} \cdot \mathbf{K} \cdot \tilde{\nabla}_z & \hat{y} \cdot \mathbf{K} \cdot \tilde{\nabla}_z & 0 \end{bmatrix} \begin{bmatrix} \overline{\tau}_x \\ \overline{\tau}_y \\ \overline{\tau}_z \end{bmatrix}$$

Asym 3,1: GM@lon=180E

Asym 3,2: GM@lon=180E



Pacific Section (180E)

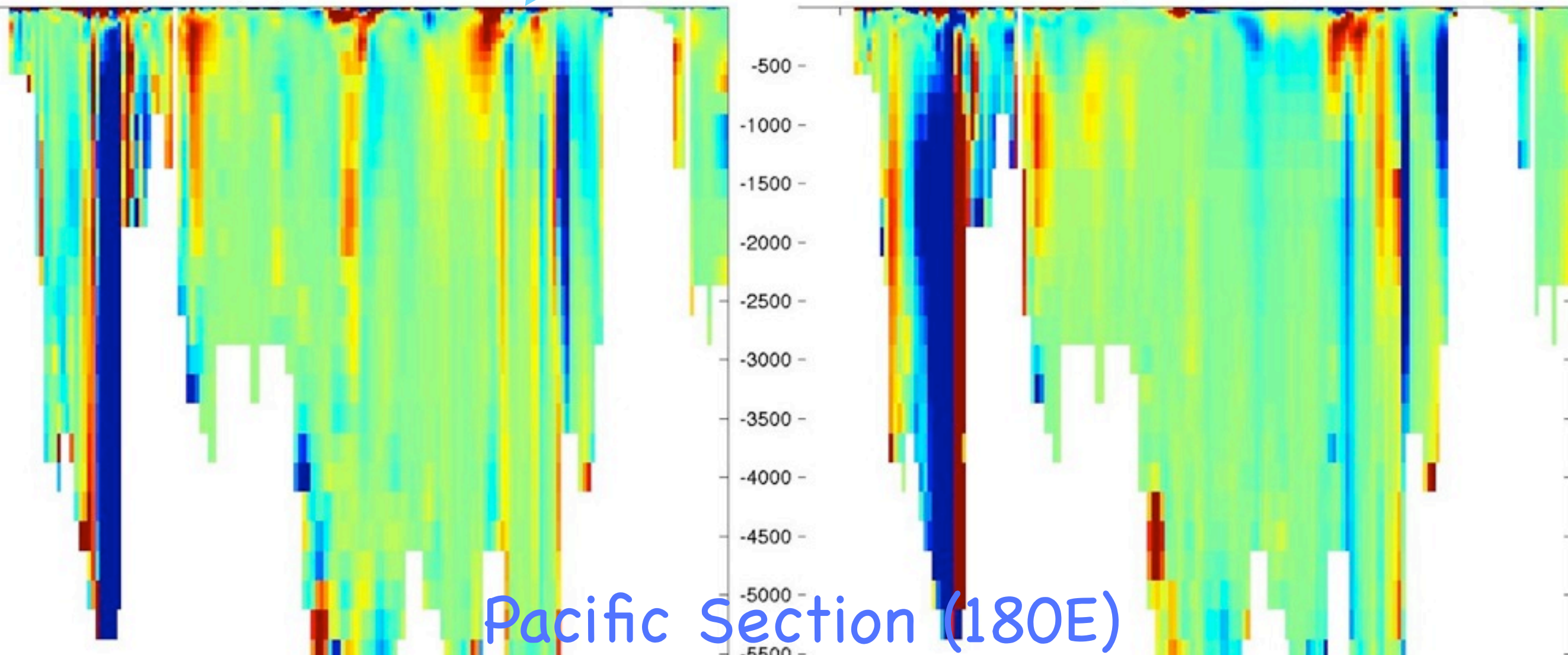


# Use a Natural, Mesoscale Eddy Environment to Test Out:

$$\begin{bmatrix} \overline{u'\tau'} \\ \overline{v'\tau'} \\ \overline{w'\tau'} \end{bmatrix} = - \begin{bmatrix} K_{xx} & K_{xy} & \hat{x} \cdot \mathbf{K} \cdot \tilde{\nabla} \mathbf{z} \\ K_{yx} & K_{yy} & \hat{y} \cdot \mathbf{K} \cdot \tilde{\nabla} \mathbf{z} \\ \hat{x} \cdot \mathbf{K} \cdot \tilde{\nabla} \mathbf{z} & \hat{y} \cdot \mathbf{K} \cdot \tilde{\nabla} \mathbf{z} & \tilde{\nabla} \mathbf{z} \cdot \mathbf{K} \cdot \tilde{\nabla} \mathbf{z} \end{bmatrix} \begin{bmatrix} \overline{\tau}_x \\ \overline{\tau}_y \\ \overline{\tau}_z \end{bmatrix}$$

Sym 3,1: Redi@lon=180E

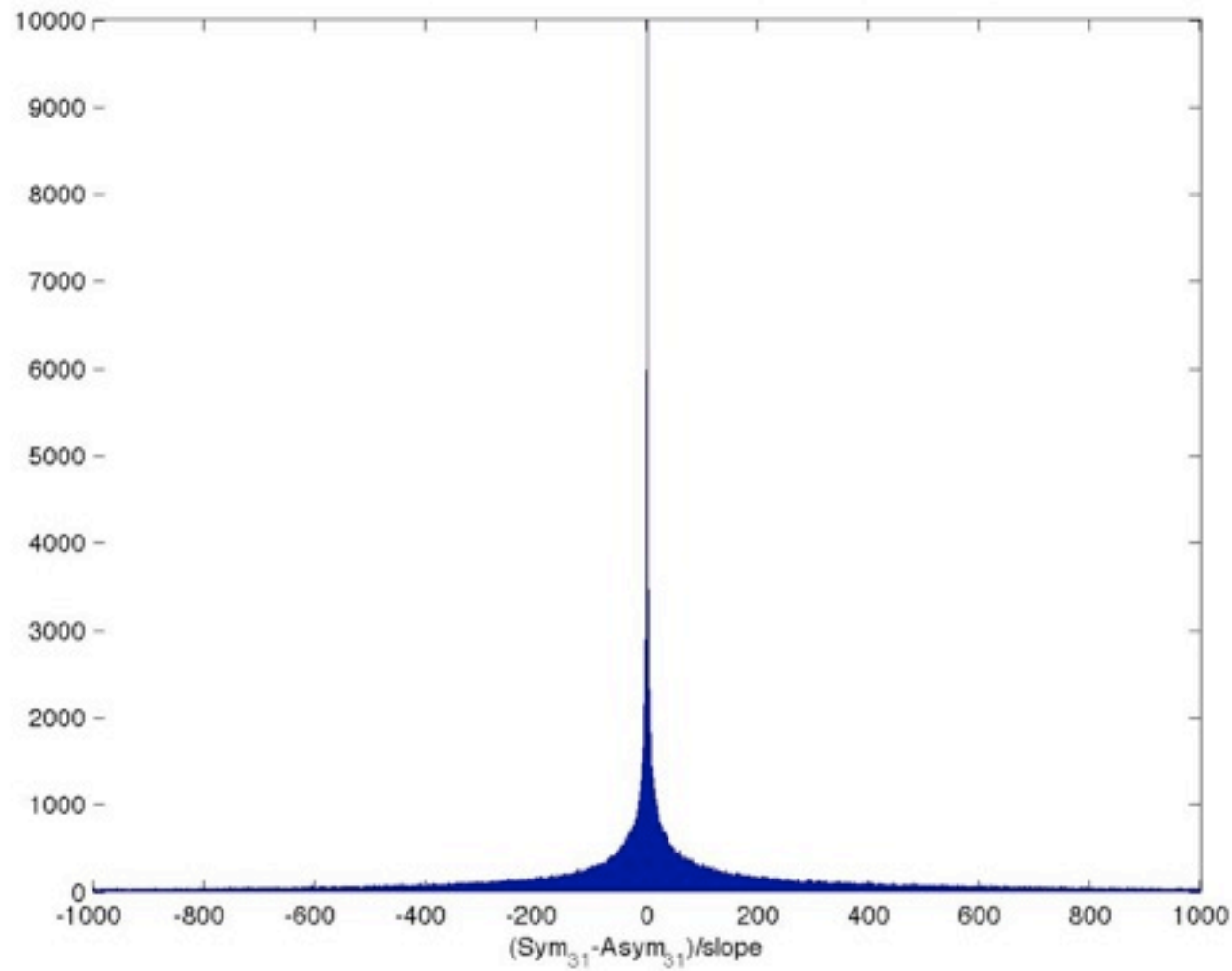
Sym 3,2: Redi@lon=180E



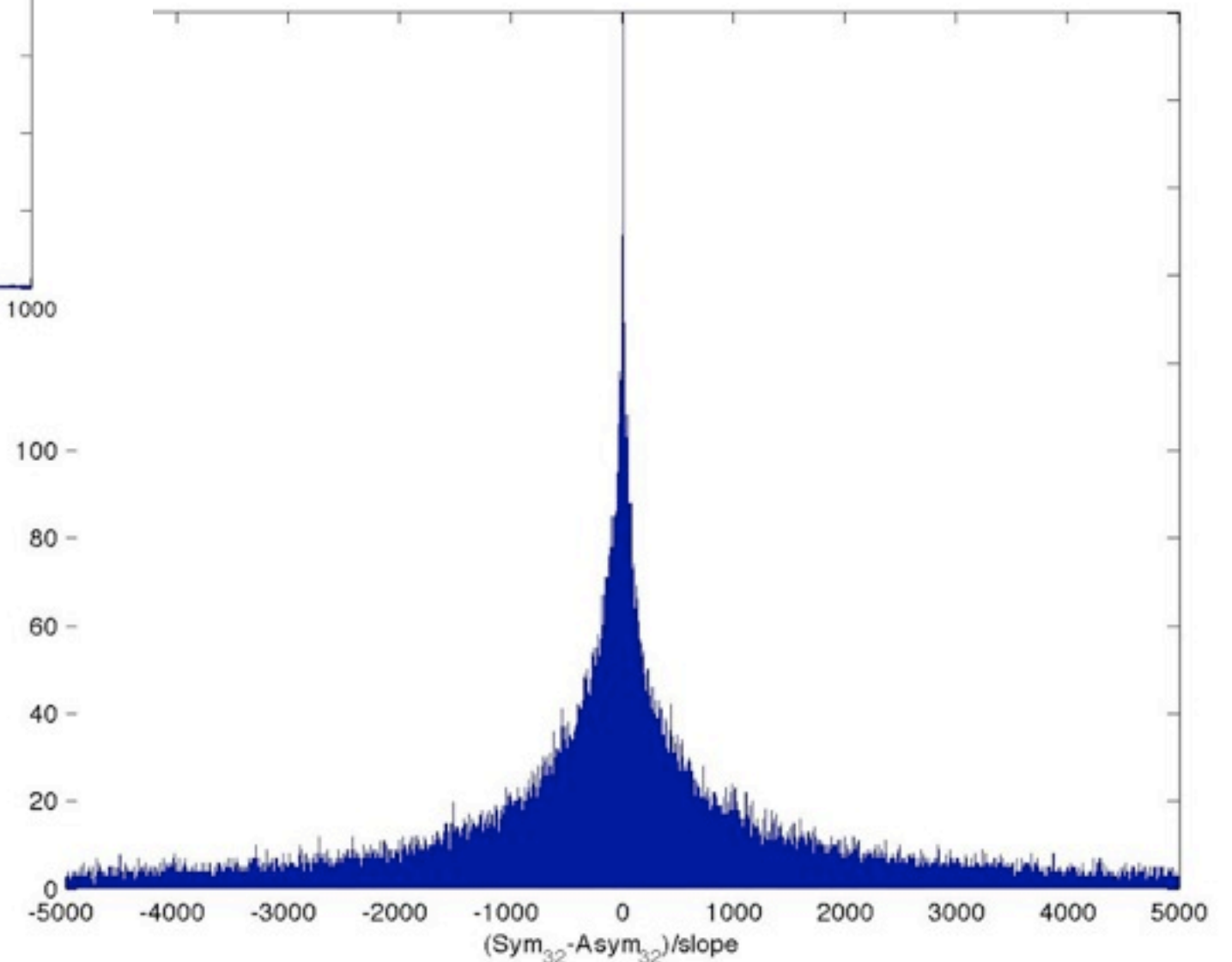


# Histograms of $|K|$

## Sym & Asym differences



These are clearly peaked near 0, but the distribution has big tails!





# NSEF & Diabatic/ Transition Layer

- Danabasoglu & Marshall
- Danabasoglu, Ferrari & McWilliams
- Ferrari, McWilliams, Canuto, Dubovikov
- Surface-intensified GM, no boundary condition issues, no over-restratification of Mixed Layer by Eddies

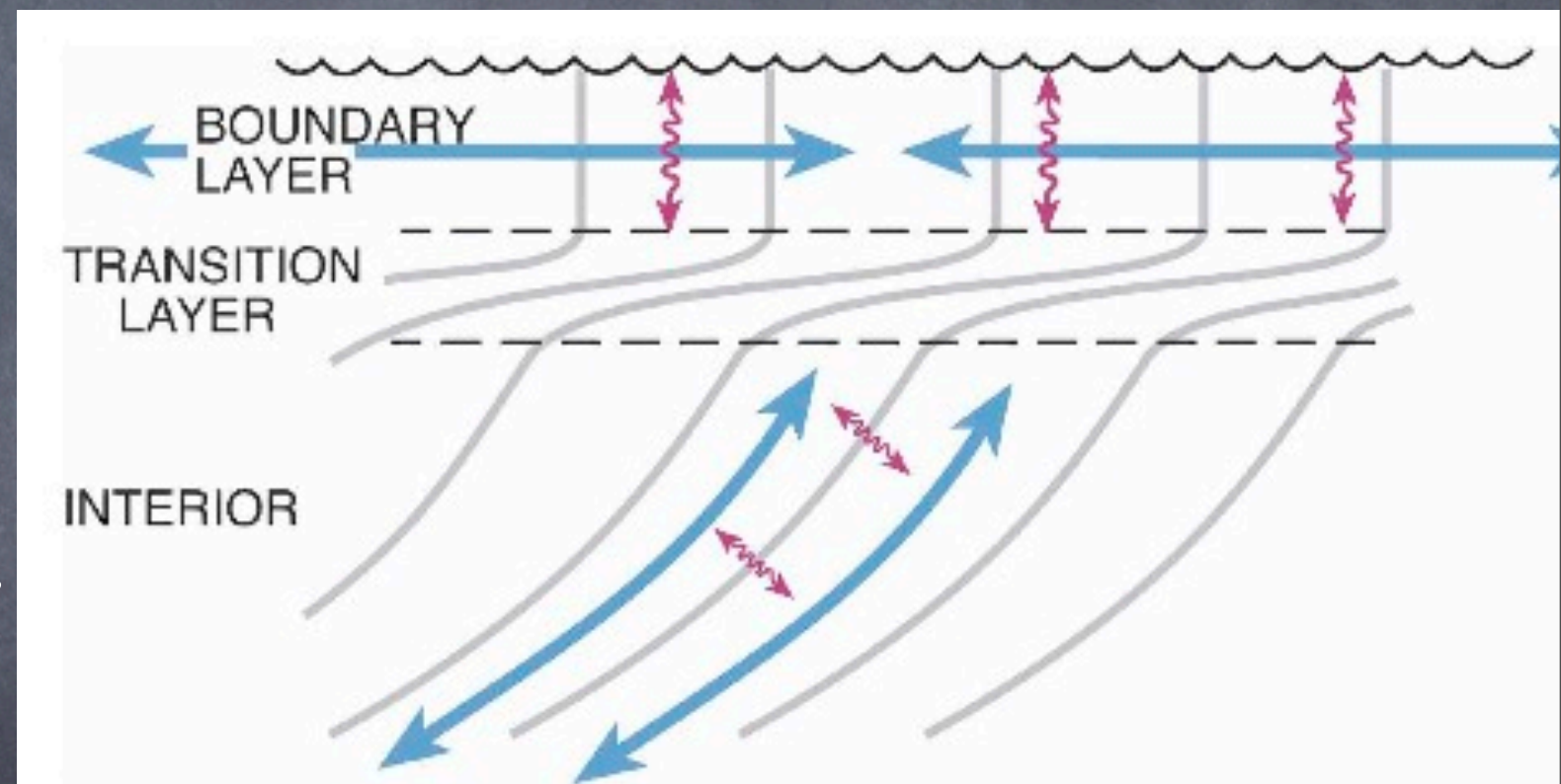
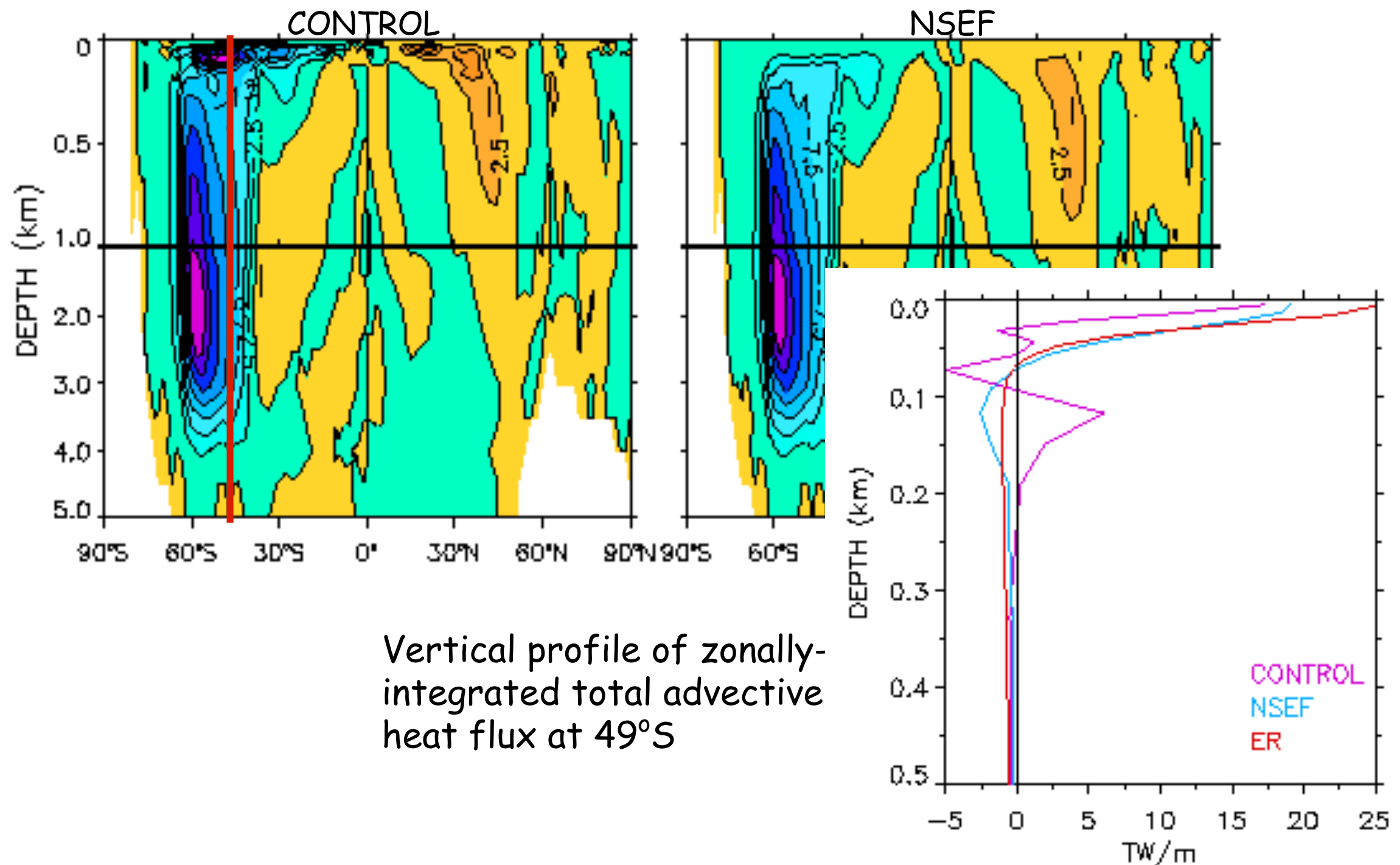


FIG. 2. A conceptual model of eddy fluxes in the upper ocean. Mesoscale eddy fluxes (blue arrows) act to both move isopycnal surfaces and stir materials along them in the oceanic interior, but the fluxes become parallel to the boundary and cross density surfaces within the *BL*. Microscale turbulent fluxes (red arrows) move



# Near-surface eddy flux scheme (Ferrari, McWilliams, Canuto, Dubovikov)

## EDDY-INDUCED MERIDIONAL OVERTURNING (GLOBAL)





# A new eddy parameterization (Ferrari, Griffies, Nurser & Vallis)

- The eddy streamfunction is given by the elliptic problem

$$\left( c^2 \frac{d^2}{dz^2} - N^2 \right) \tilde{\Psi} = -\kappa \nabla \bar{b}$$
$$\tilde{\Psi} = 0, \quad z = 0, -H$$

Properties of the new parameterization

- releases mean available potential energy
- the eddy transport vanishes at the ocean boundaries
- the eddy transport is dominated by the first baroclinic mode (if  $c$  is set to speed of first baroclinic mode)
- does not require any tapering function
- reduces to GM for  $c=0$



# Eden, Jochum, Danabasoglu:

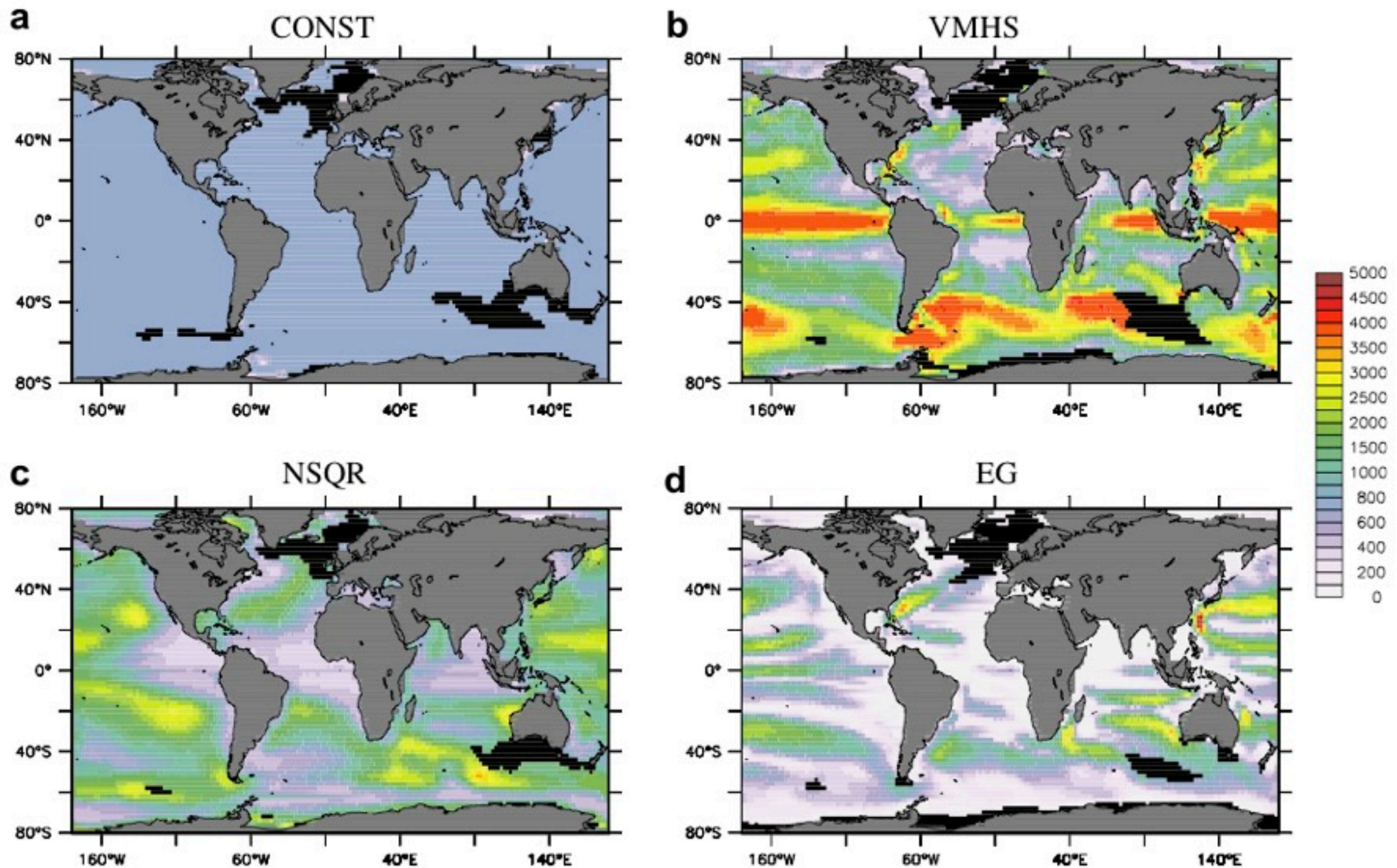
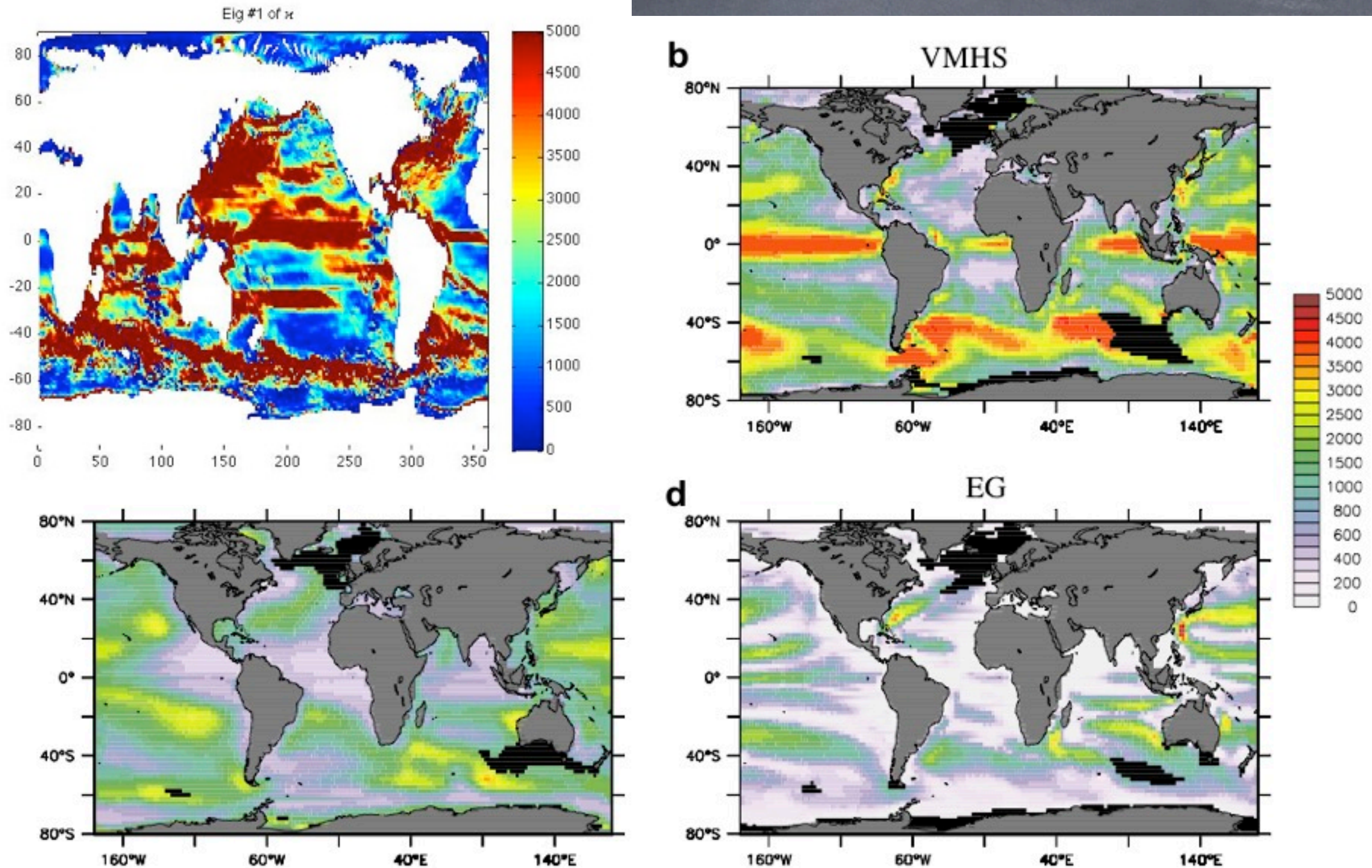


Fig. 1. Annual mean thickness diffusivity ( $K$ ) in  $m^2/s$  at 300 m depth in experiment CONST (a), VMHS (b), NSQR (c) and EG (d) after 500 years integration. Values of  $K$  are shown for the interior region only, i.e. values of  $K$  in the (seasonal maximum) diabatic surface and transition layer are not shown and shaded black. Note the non-linear colour scale for the thickness diffusivity. Note also that the data have been interpolated from the model grid to a regular rectangular grid of similar resolution prior to plotting. The land mask in the figure (taken from Smith and Sandwell (1997)) differs therefore slightly from the model's land mask.



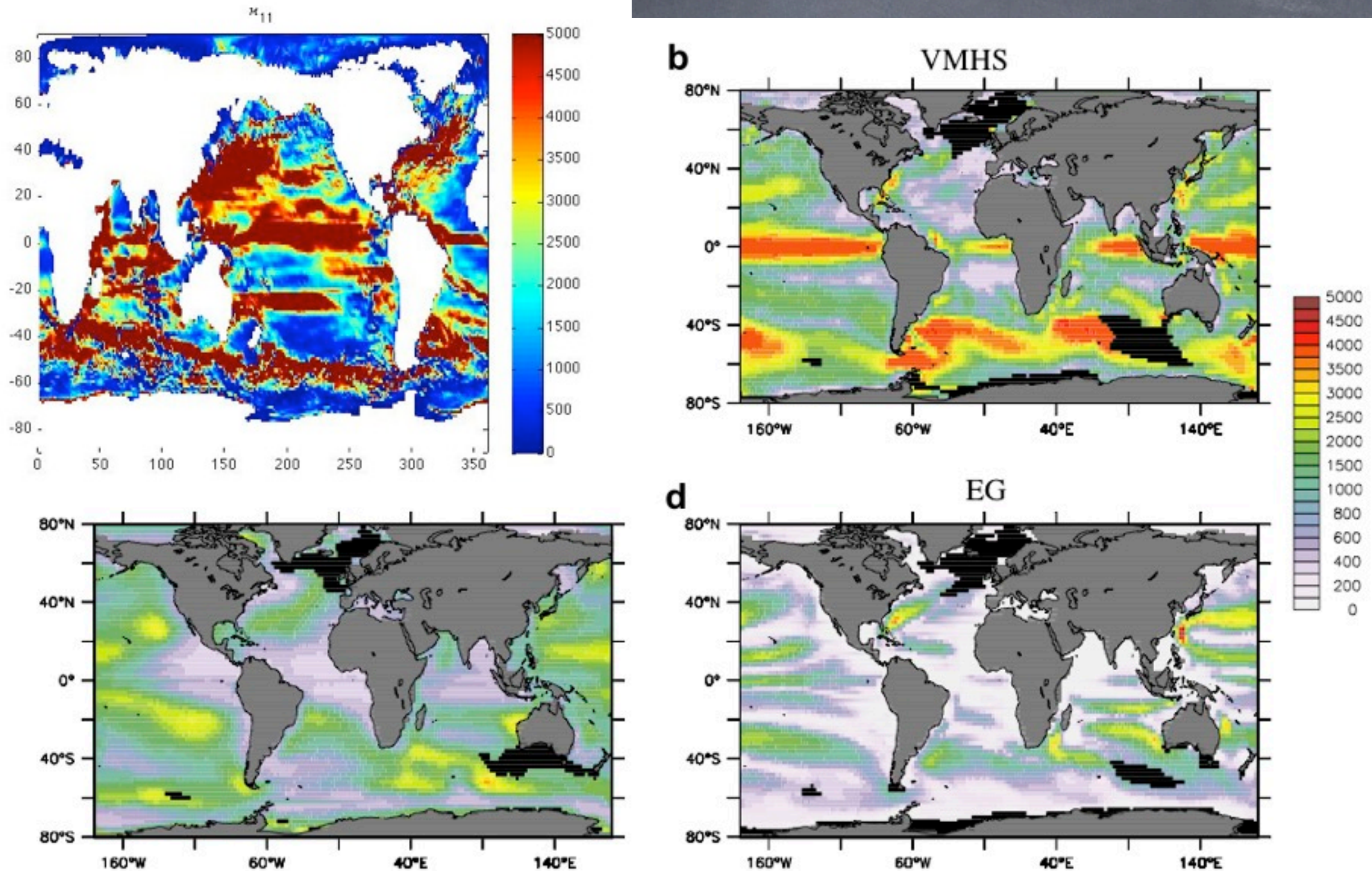
# Eden, Jochum, Danabasoglu vs. Eigenvalue #1



**Fig. 1.** Annual mean thickness diffusivity ( $K$ ) in  $\text{m}^2/\text{s}$  at 300 m depth in experiment CONST (a), VMHS (b), NSQR (c) and EG (d) after 500 years integration. Values of  $K$  are shown for the interior region only, i.e. values of  $K$  in the (seasonal maximum) diabatic surface and transition layer are not shown and shaded black. Note the non-linear colour scale for the thickness diffusivity. Note also that the data have been interpolated from the model grid to a regular rectangular grid of similar resolution prior to plotting. The land mask in the figure (taken from Smith and Sandwell (1997)) differs therefore slightly from the model's land mask.



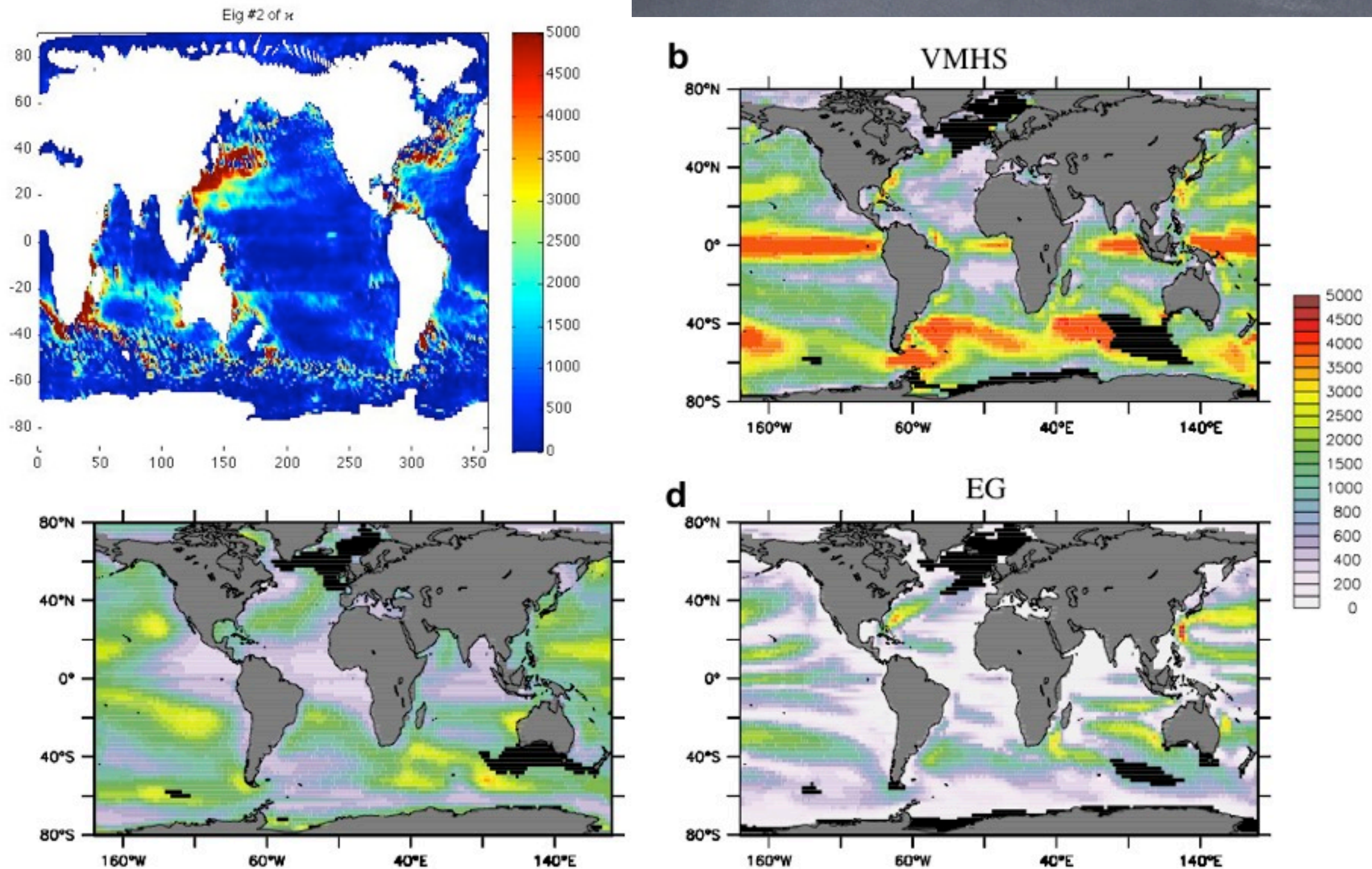
# Eden, Jochum, Danabasoglu vs. $M_{22}$



**Fig. 1.** Annual mean thickness diffusivity ( $K$ ) in  $m^2/s$  at 300 m depth in experiment CONST (a), VMHS (b), NSQR (c) and EG (d) after 500 years integration. Values of  $K$  are shown for the interior region only, i.e. values of  $K$  in the (seasonal maximum) diabatic surface and transition layer are not shown and shaded black. Note the non-linear colour scale for the thickness diffusivity. Note also that the data have been interpolated from the model grid to a regular rectangular grid of similar resolution prior to plotting. The land mask in the figure (taken from Smith and Sandwell (1997)) differs therefore slightly from the model's land mask.



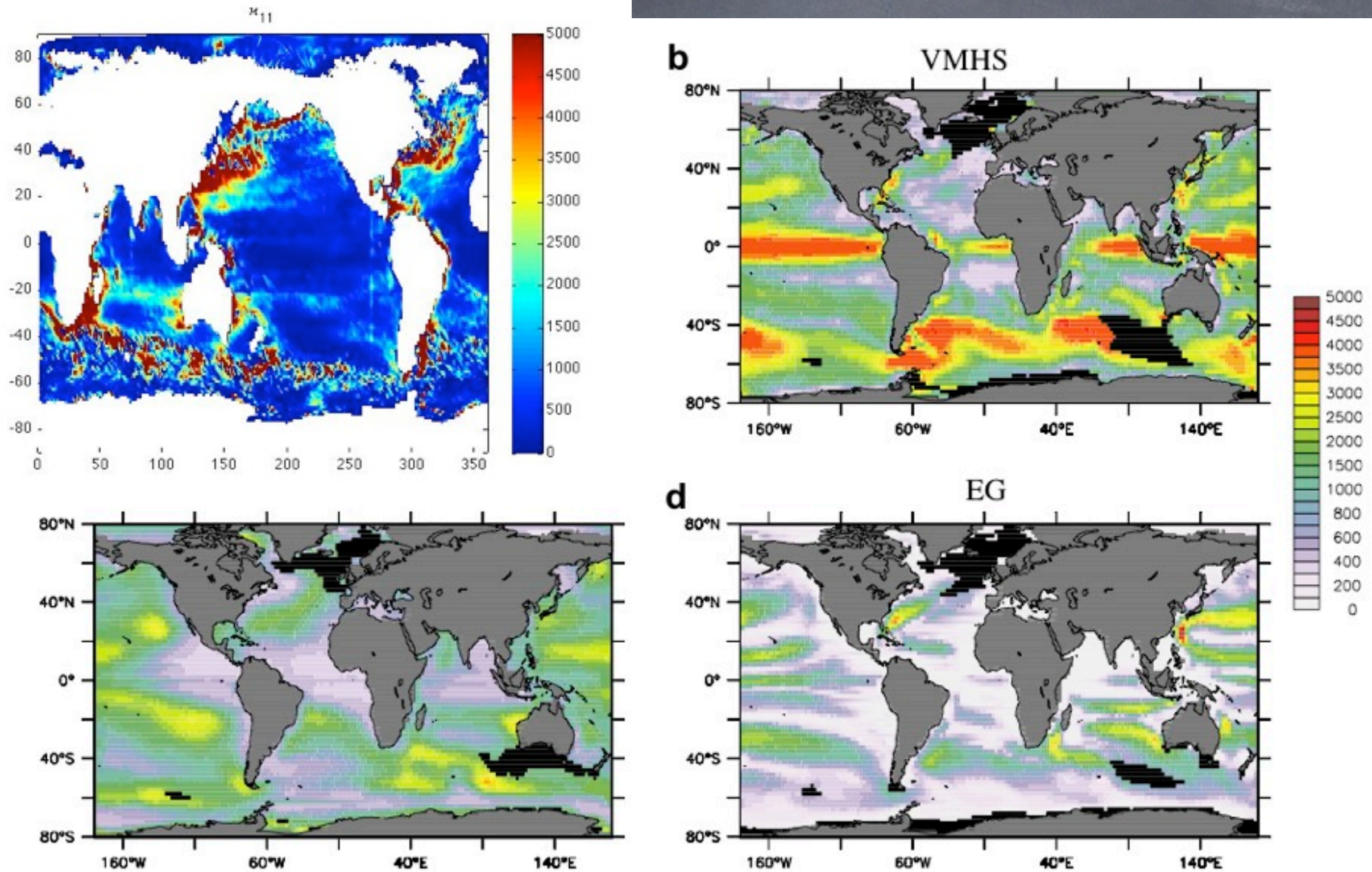
# Eden, Jochum, Danabasoglu vs. Eigenvalue #2



**Fig. 1.** Annual mean thickness diffusivity ( $K$ ) in  $\text{m}^2/\text{s}$  at 300 m depth in experiment CONST (a), VMHS (b), NSQR (c) and EG (d) after 500 years integration. Values of  $K$  are shown for the interior region only, i.e. values of  $K$  in the (seasonal maximum) diabatic surface and transition layer are not shown and shaded black. Note the non-linear colour scale for the thickness diffusivity. Note also that the data have been interpolated from the model grid to a regular rectangular grid of similar resolution prior to plotting. The land mask in the figure (taken from Smith and Sandwell (1997)) differs therefore slightly from the model's land mask.

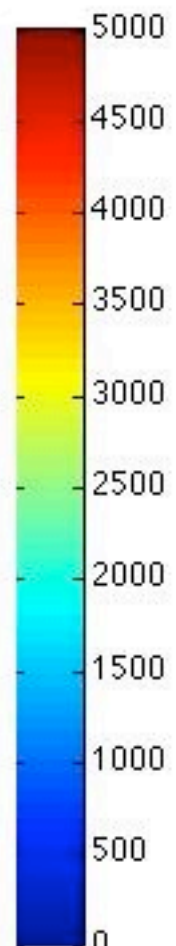
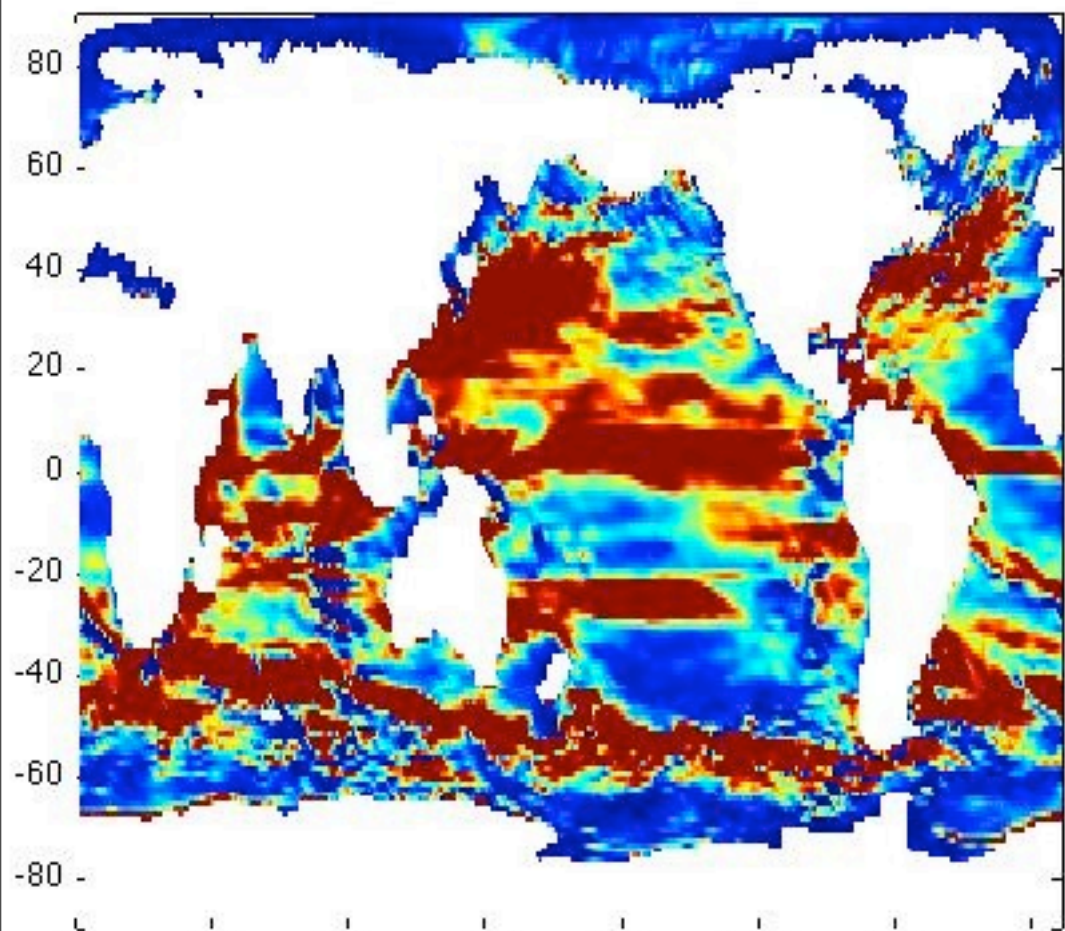
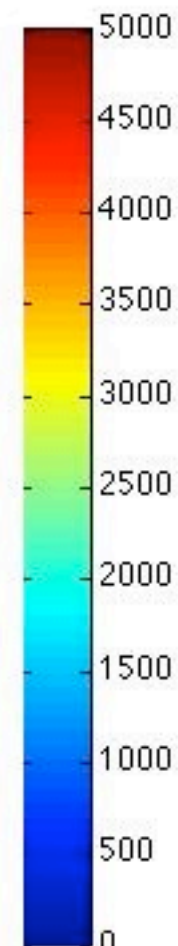
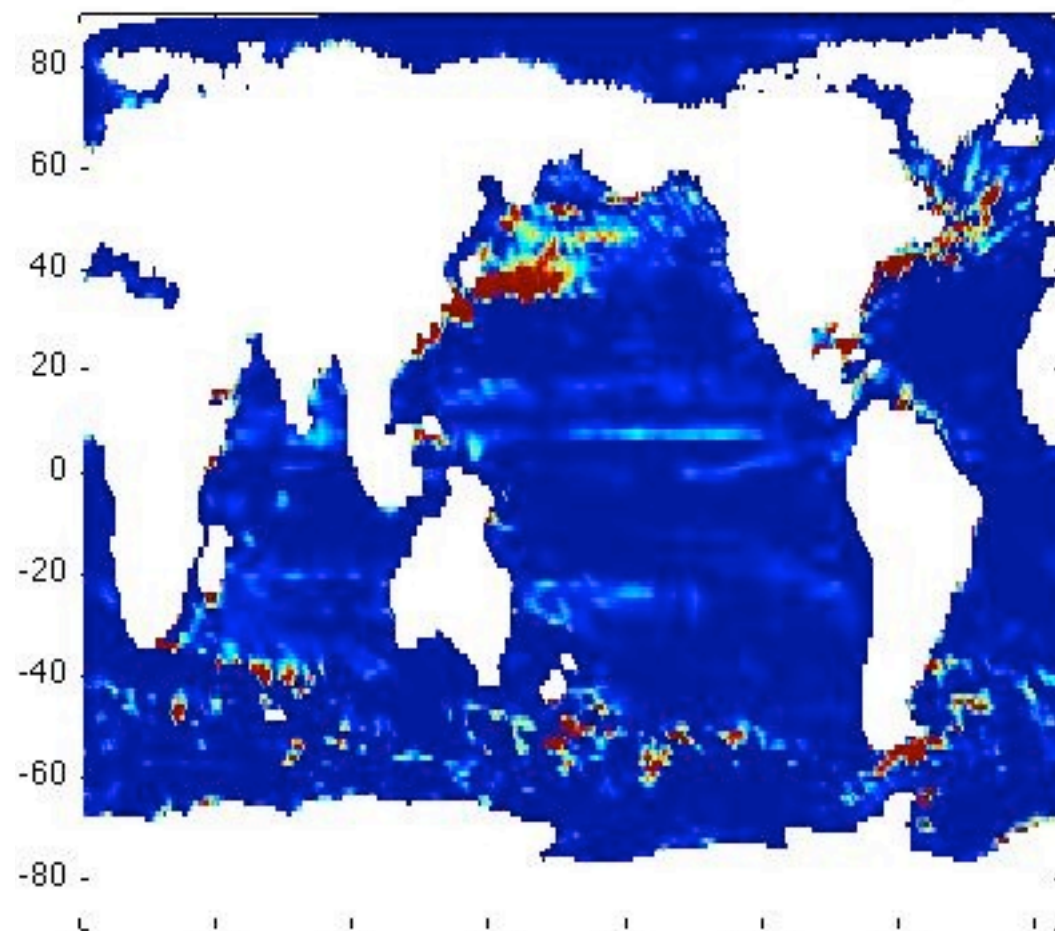
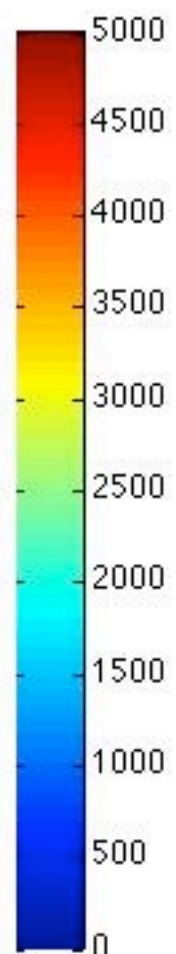
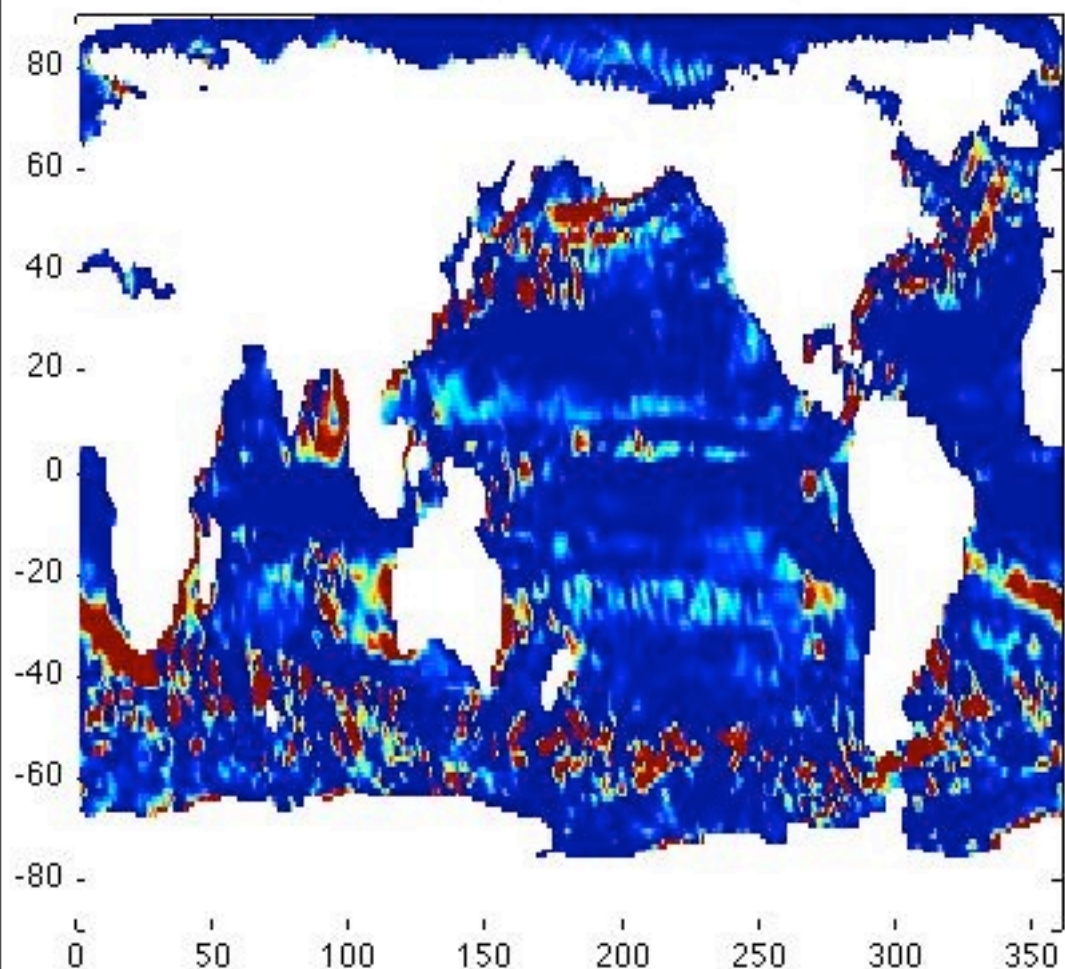
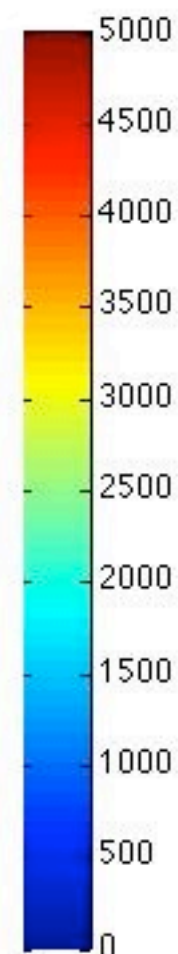
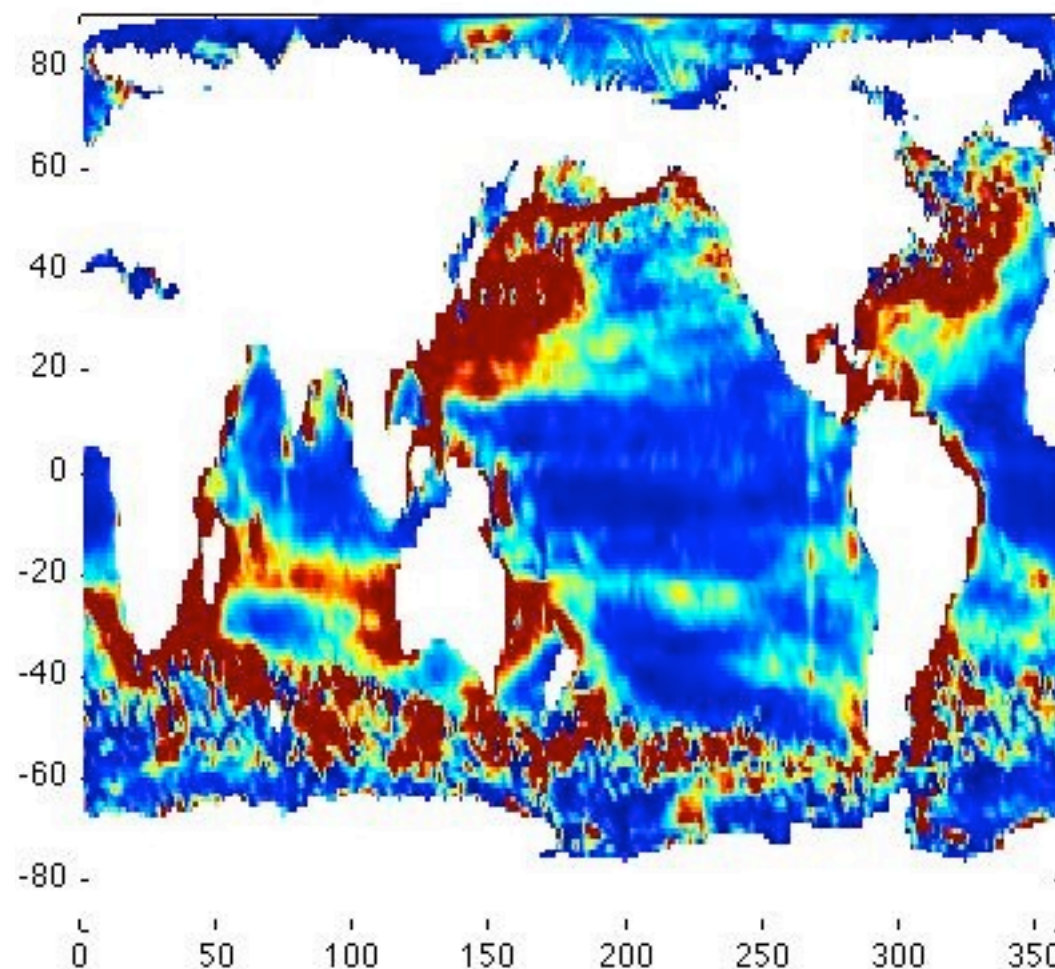


# Eden, Jochum, Danabasoglu vs. $M_{11}$

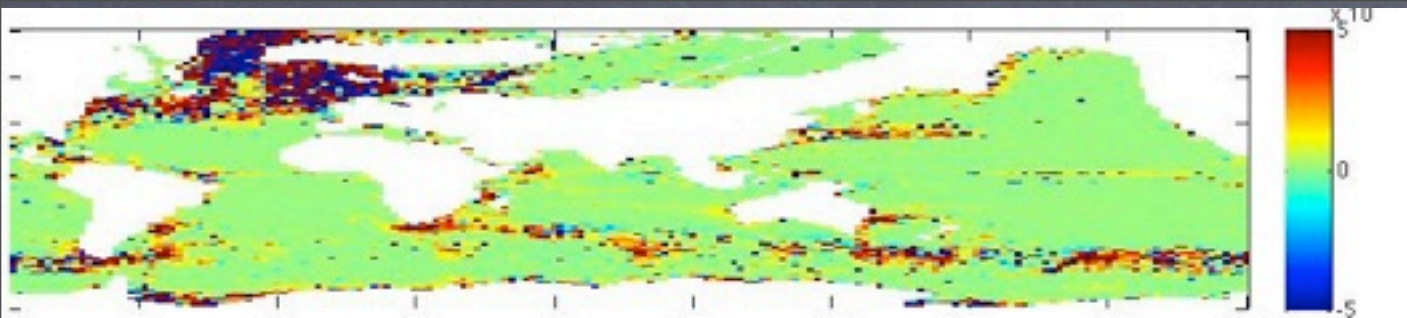


**Fig. 1.** Annual mean thickness diffusivity ( $K$ ) in  $m^2/s$  at 300 m depth in experiment CONST (a), VMHS (b), NSQR (c) and EG (d) after 500 years integration. Values of  $K$  are shown for the interior region only, i.e. values of  $K$  in the (seasonal maximum) diabatic surface and transition layer are not shown and shaded black. Note the non-linear colour scale for the thickness diffusivity. Note also that the data have been interpolated from the model grid to a regular rectangular grid of similar resolution prior to plotting. The land mask in the figure (taken from Smith and Sandwell (1997)) differs therefore slightly from the model's land mask.



$\kappa_{11}$  $\kappa_{12}$  $\kappa_{21}$  $\kappa_{22}$ 





# Conclusions

- Passive Tracers are used in a **global 0.1 model** to **diagnose Mesoscale Flux-Gradient Relationship**
- **Resembles  $GM \approx Redi$**  with  $O(500 \text{ to } 2000 \text{m}^2/\text{s})$  at 150m depth, but long tails...)
- Strongly **anisotropic** (mostly zonal, strong flow)
- **Depth-dependent Streamfunction: MLB intensified** changes behavior in diabatic/mixed layer
- **K does not scale well with Mean KE or  $N^2$**
- Active vs. Passive tracers apparently not an issue
- **$M_{zx}$  &  $M_{xz}$  are  $O(\text{along-iso})$** , detailed contrast later



# Comparisons with Marshall et al.

Ferreira, Marshall, Heimbach 05

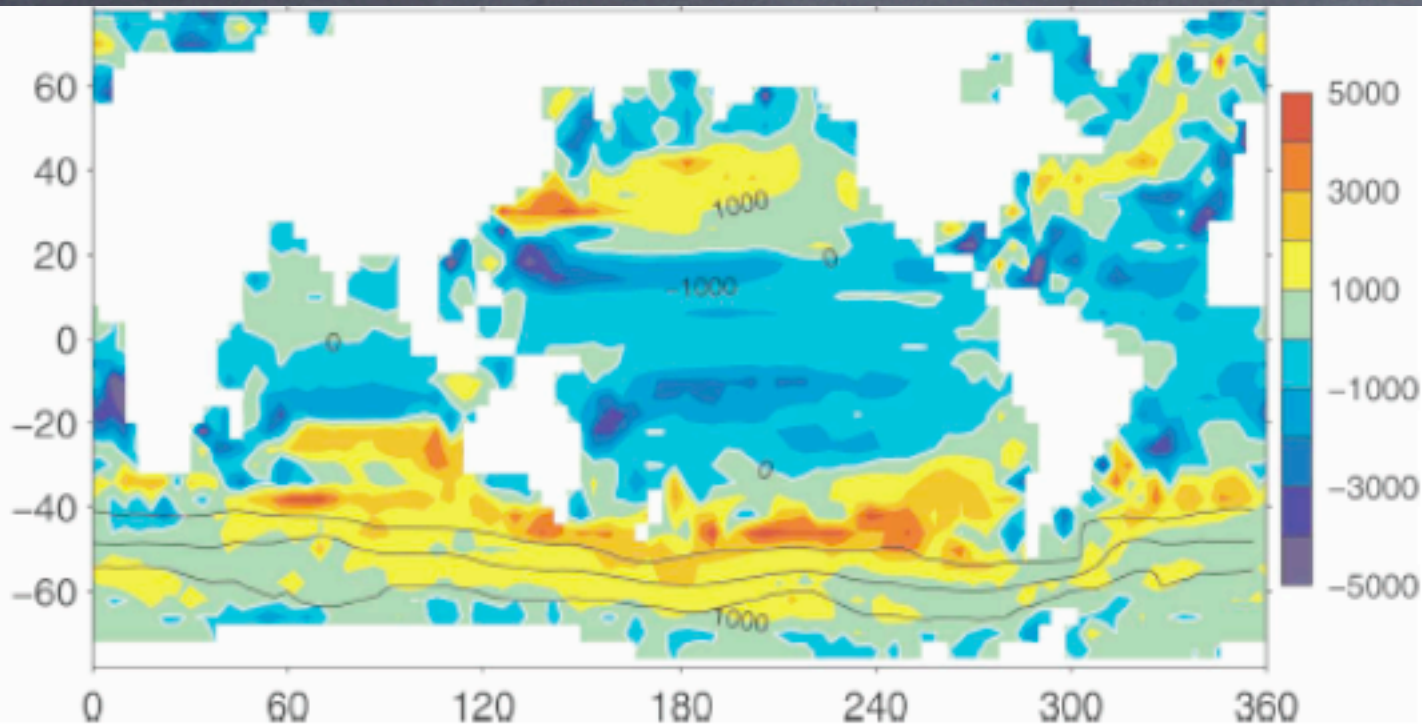
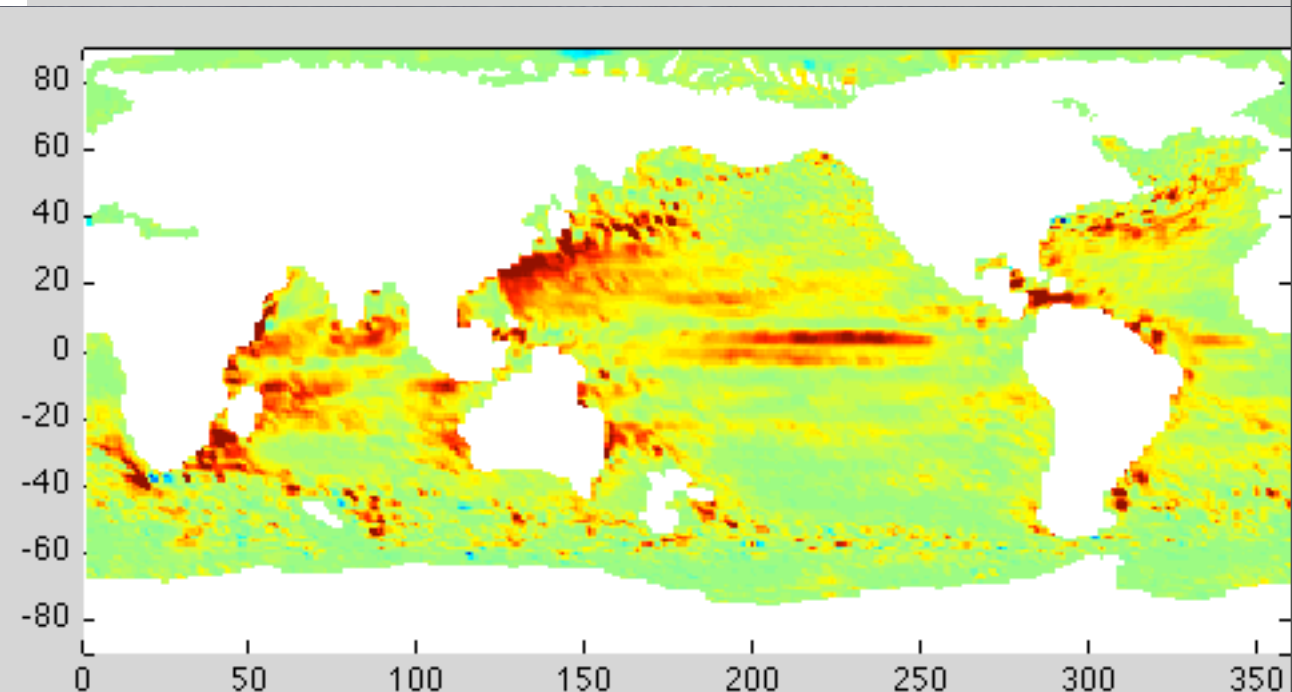
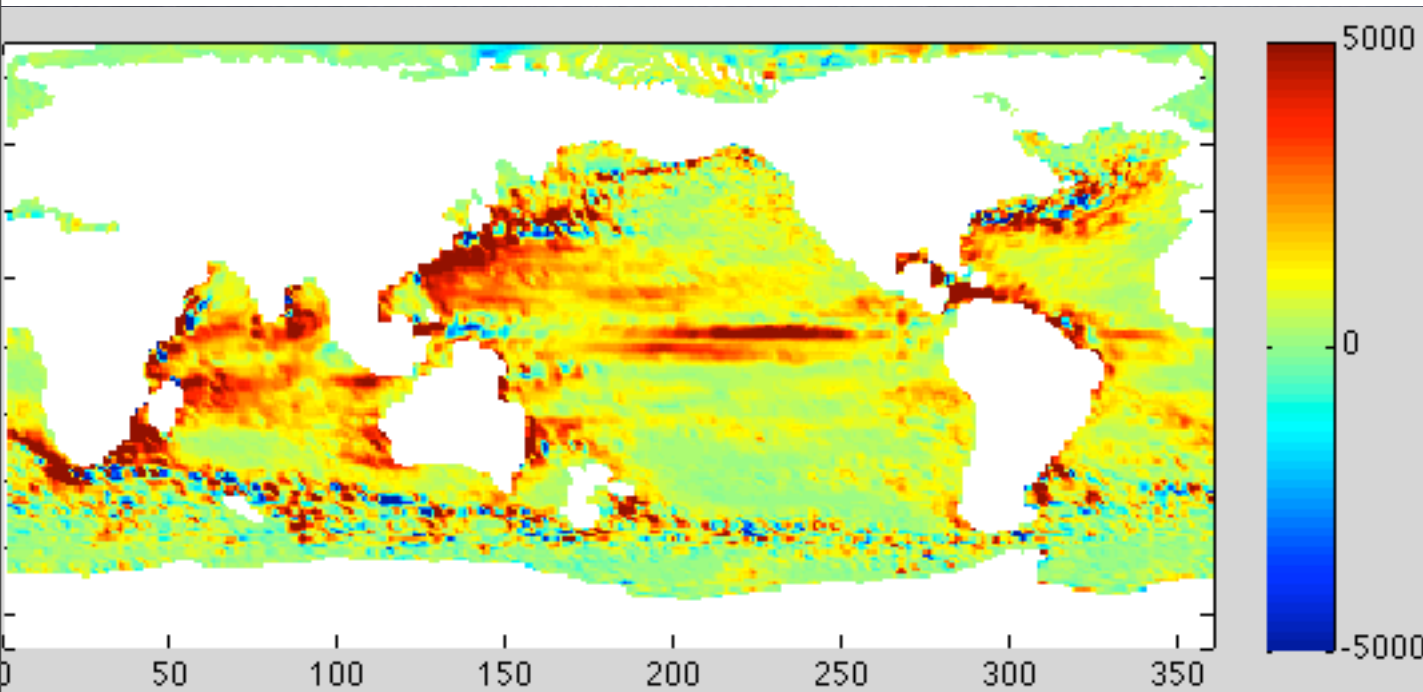
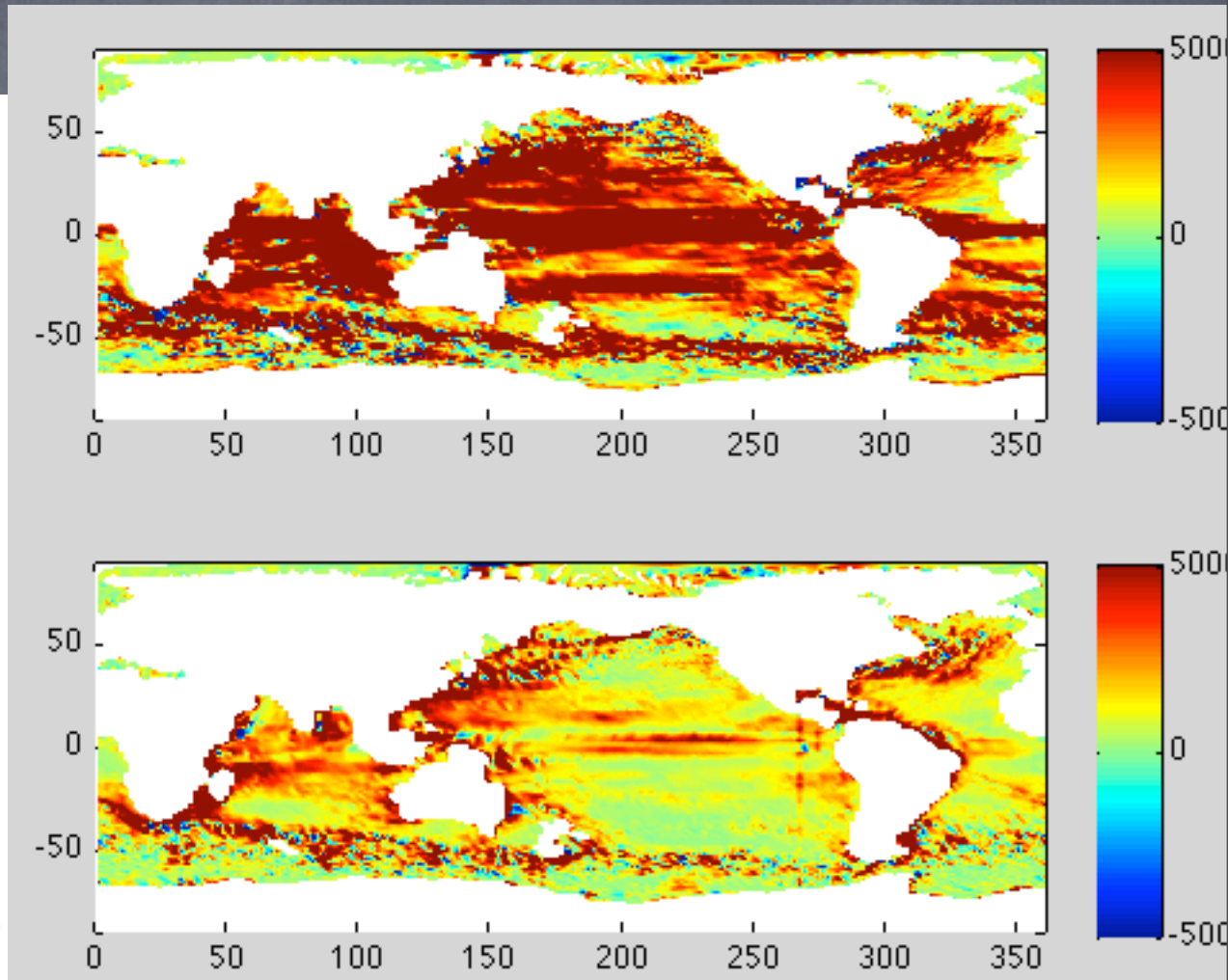


FIG. 12. Inferred horizontal eddy diffusivity  $\kappa$  ( $\text{m}^2 \text{s}^{-1}$ ): (top) zonal mean and (bottom) vertical mean over the thermocline (0–1200 m). The contour intervals are (top) 500 and (bottom) 1000  $\text{m}^2 \text{s}^{-1}$ . The thick line indicates the zero contour. Also indicated in the bottom panel are the 10-, 70-, and 130-Sv contours of the barotropic streamfunction.

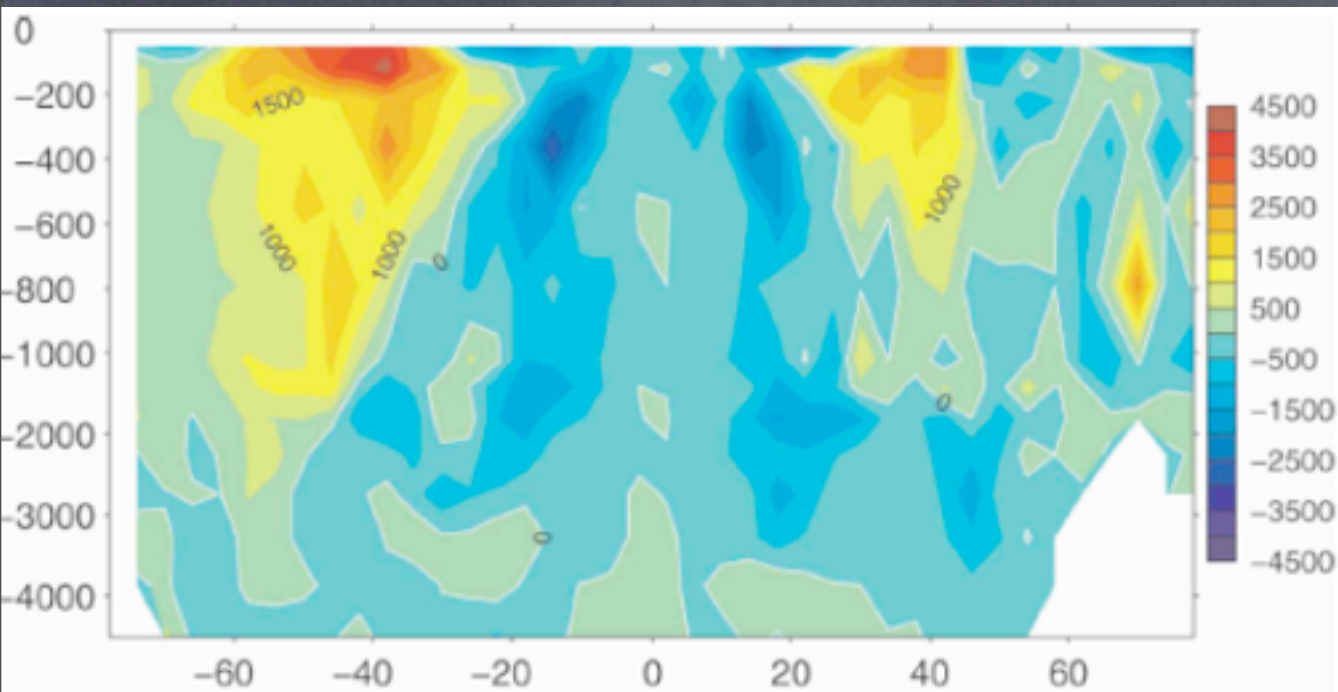


Re(2nd eigenvalue)

(2nd eigenvalue of symmetric M)



# Comparisons with Marshall et al.

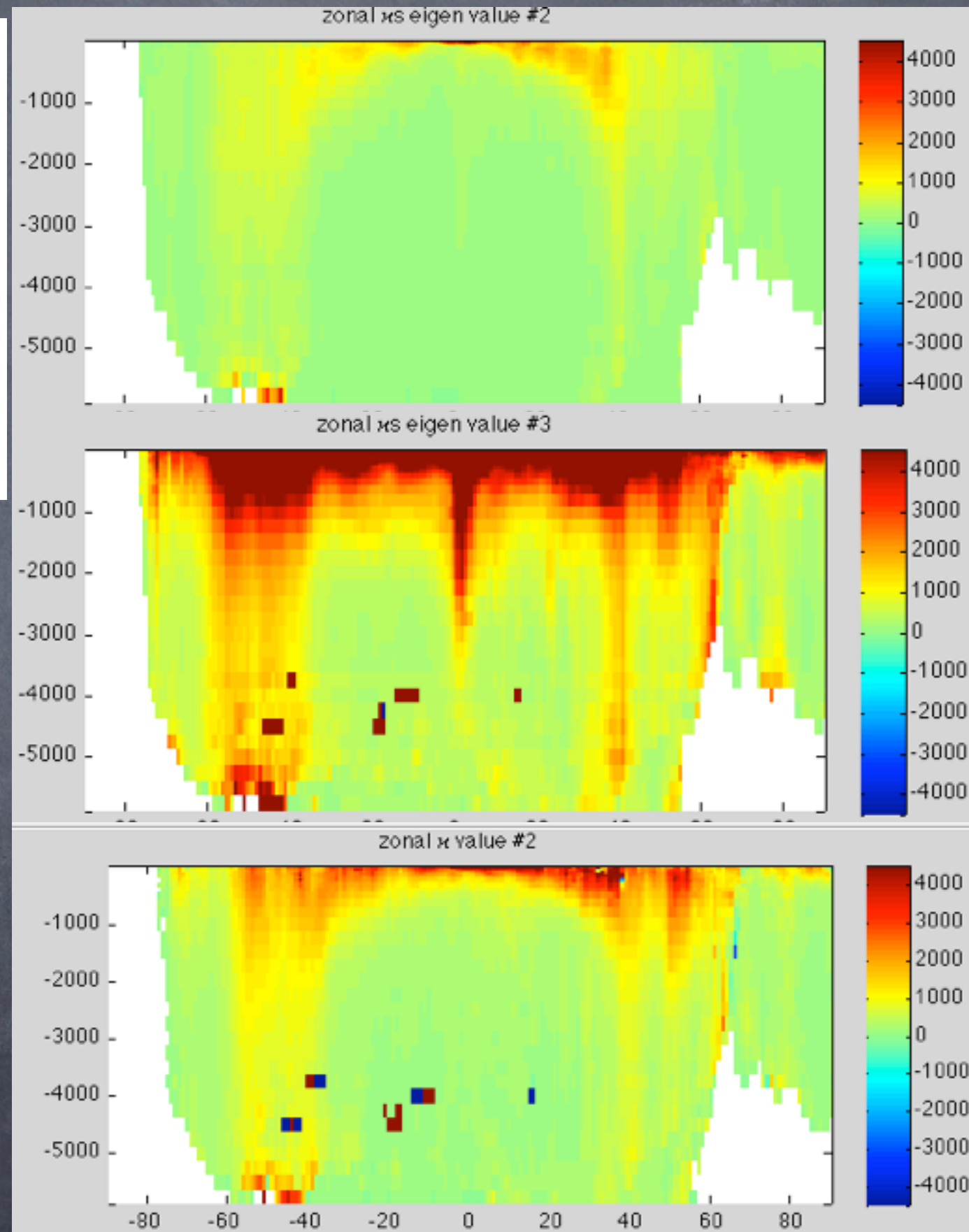


Ferreira, Marshall, Heimbach 05

Zonal mean (scalar) diffusivity  
vs.

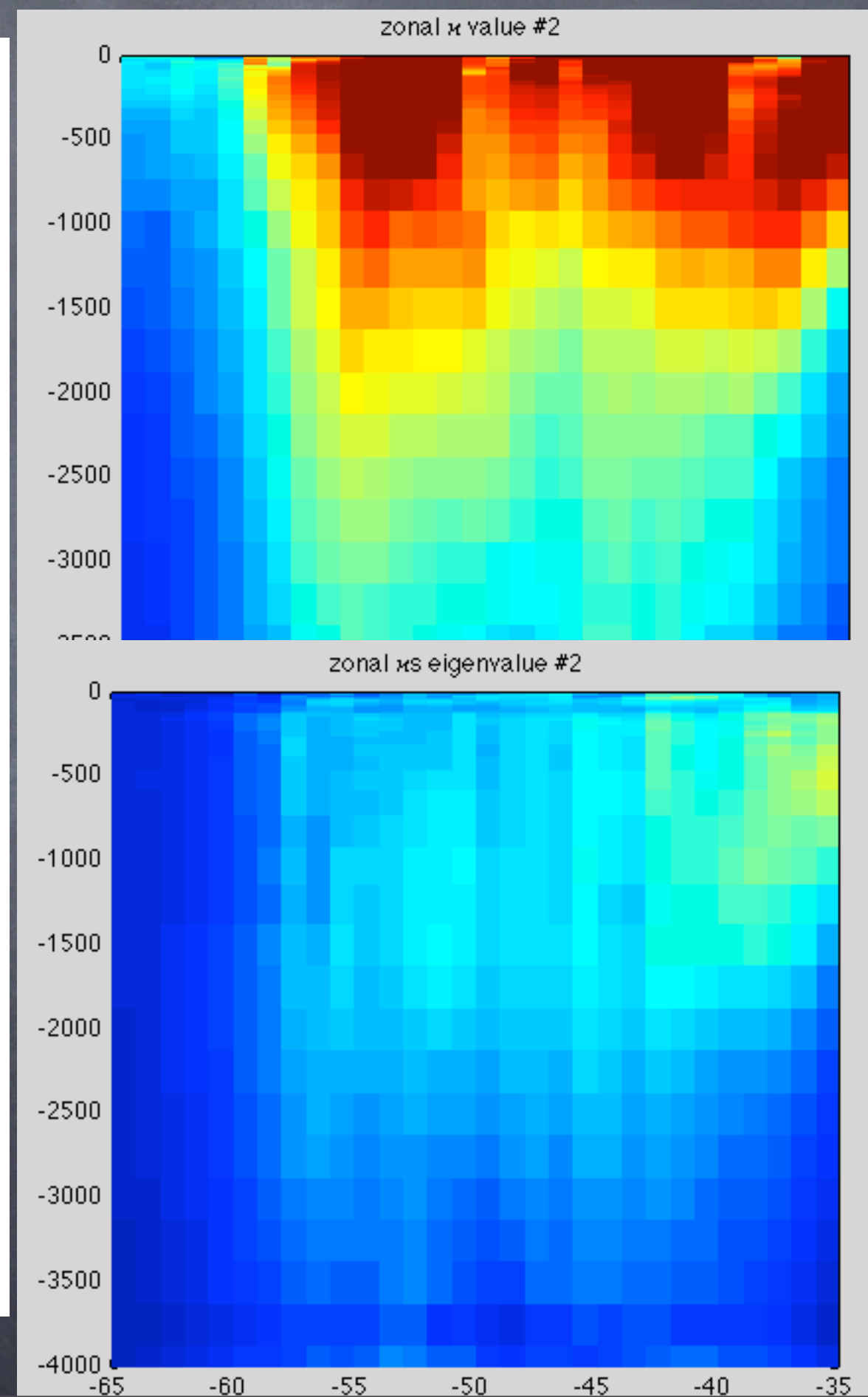
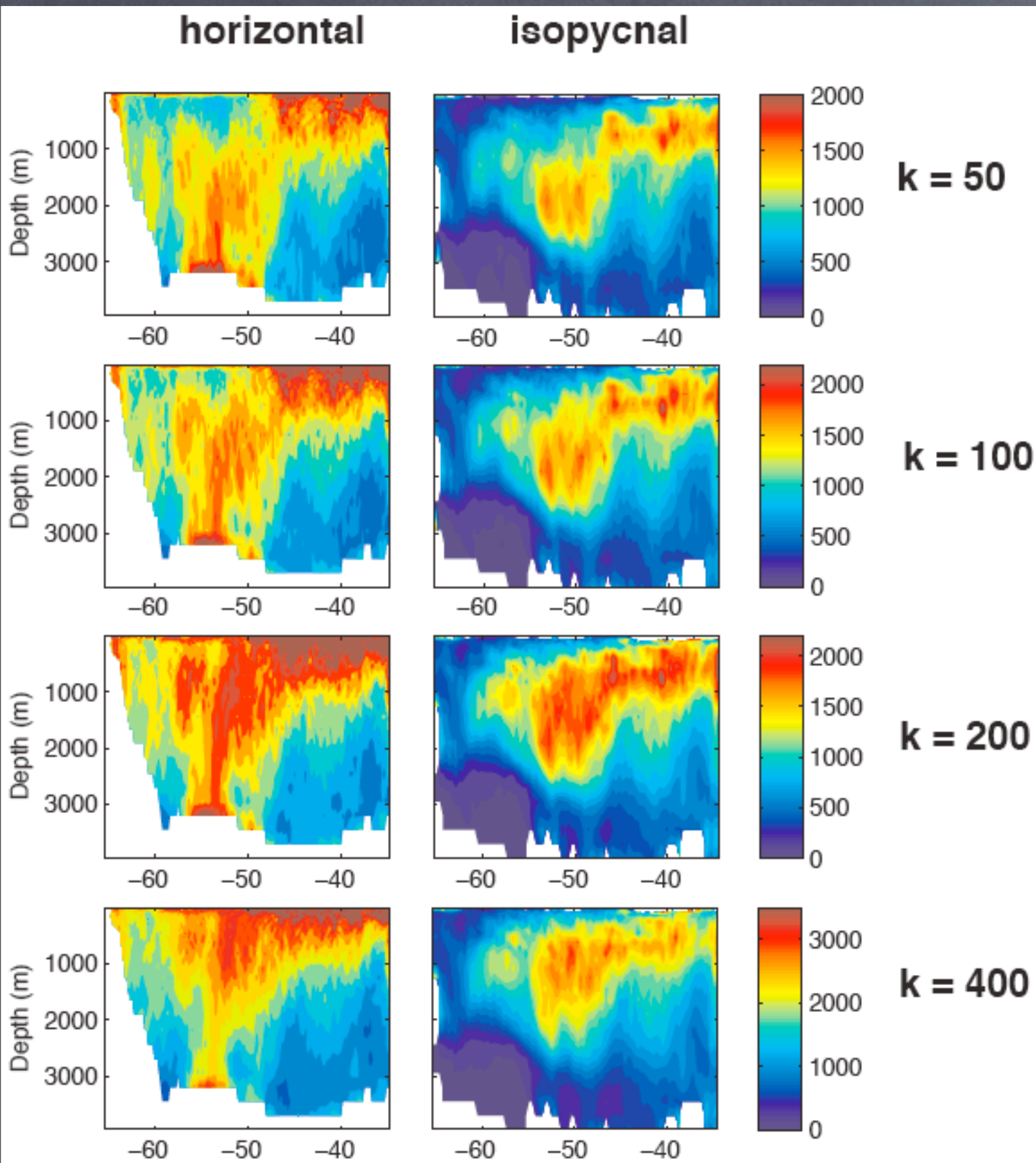
Eigenvalues of the symmetric  
tensor

Same shape--no negatives!





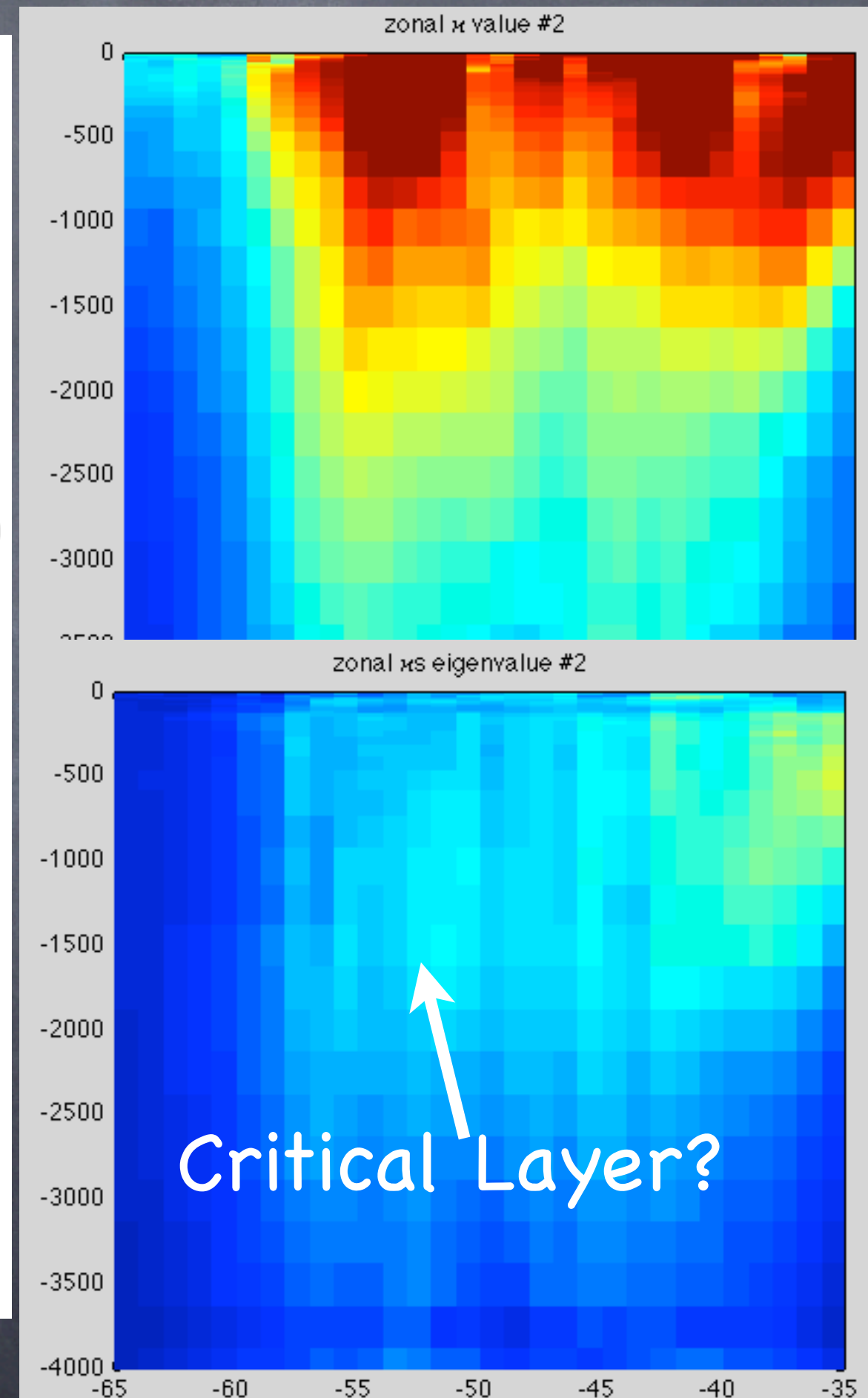
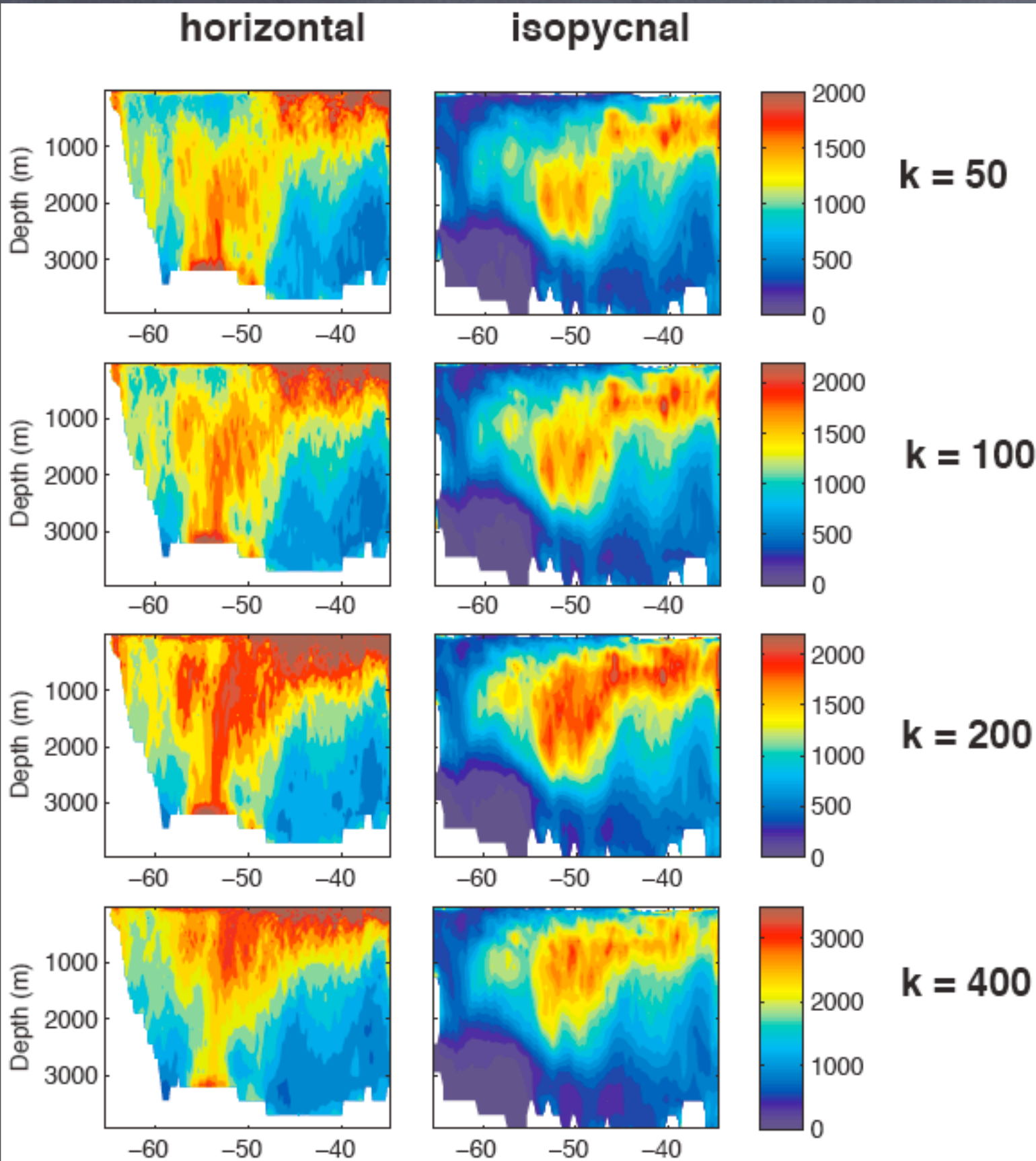
# Comparisons with Marshall et al.



Abernathy et al 09



# Comparisons with Marshall et al.



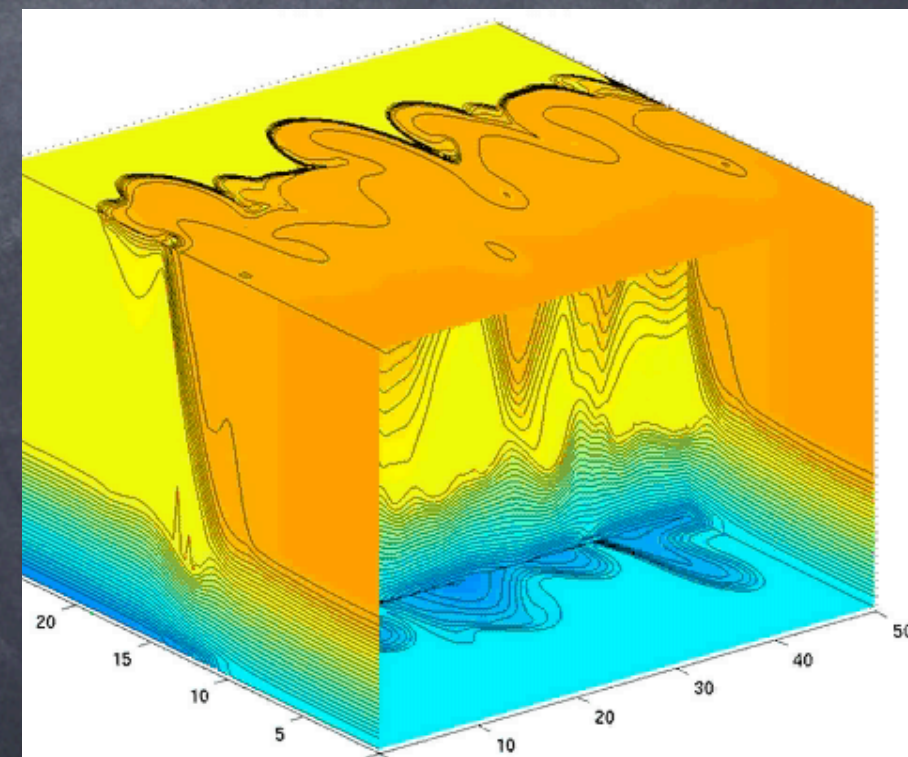
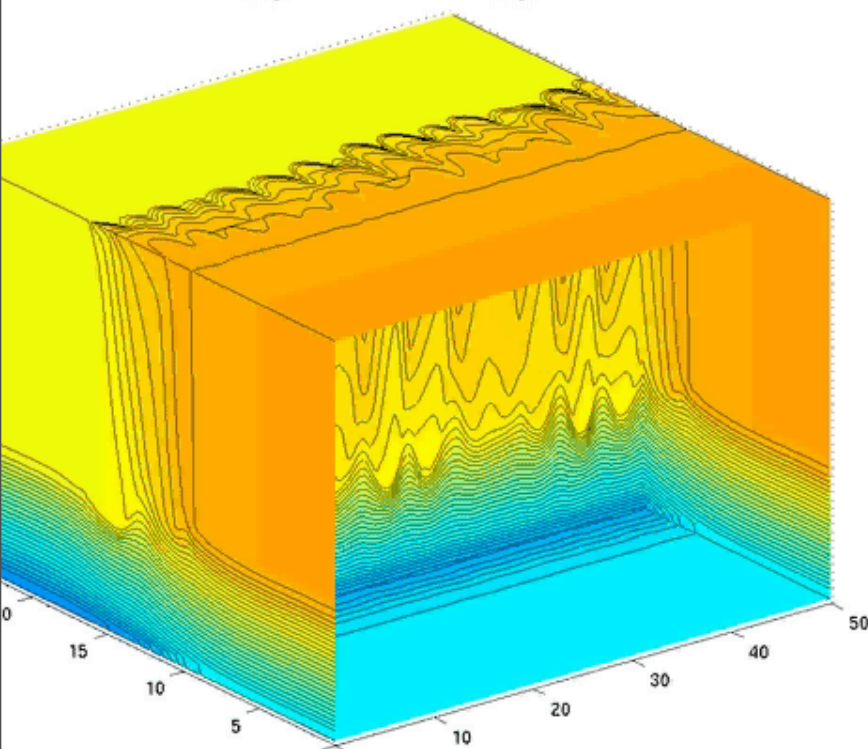
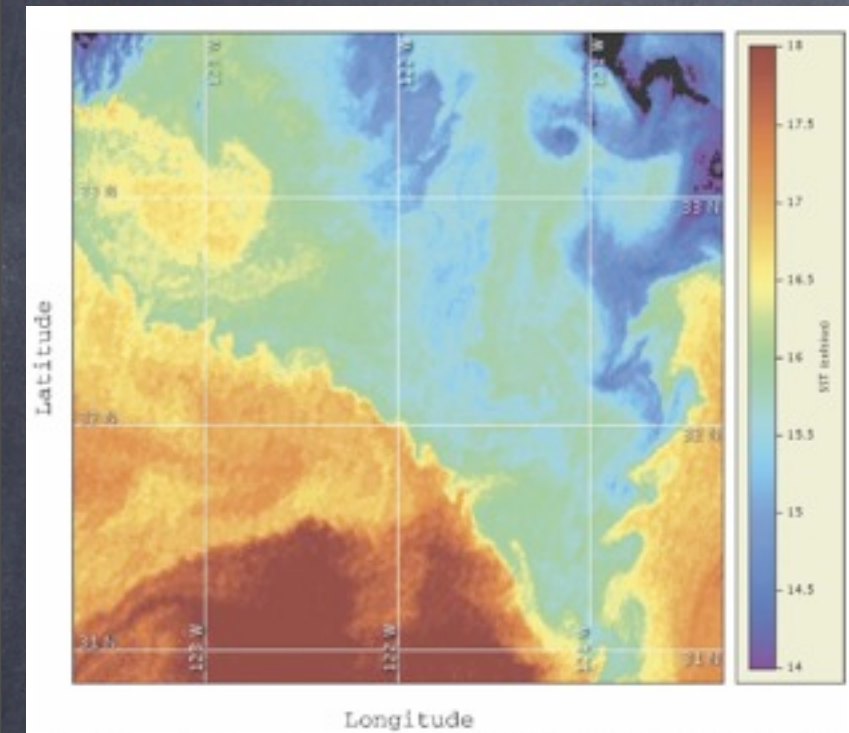
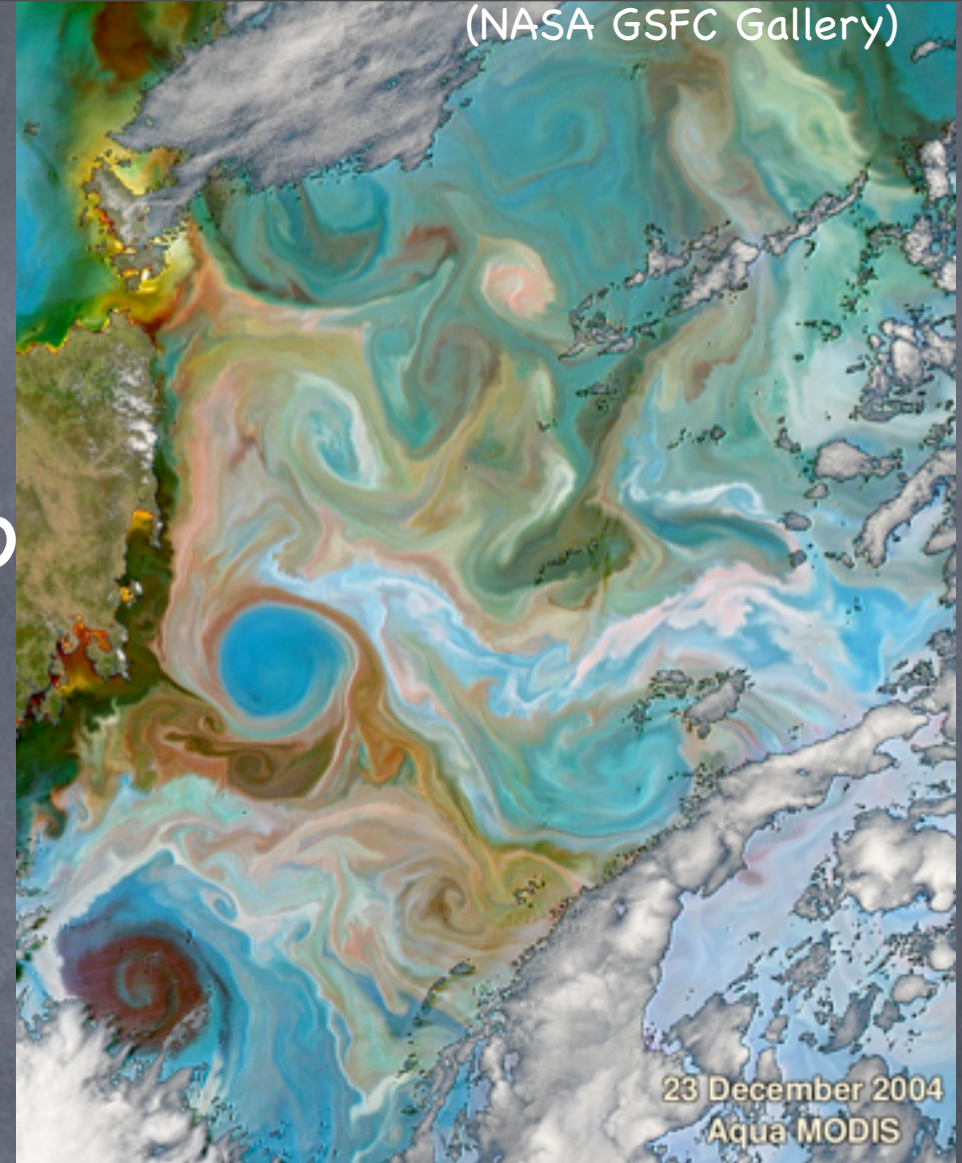
Abernathy et al 09



# The Character of the Submesoscale

(Capet et al., 2008)

- Fronts & ageo wind
- Eddies
- $Ro=O(1)$
- $Ri=O(1)$
- near-surface
- 10km, days
- Parameterizations of eddies (FFH)

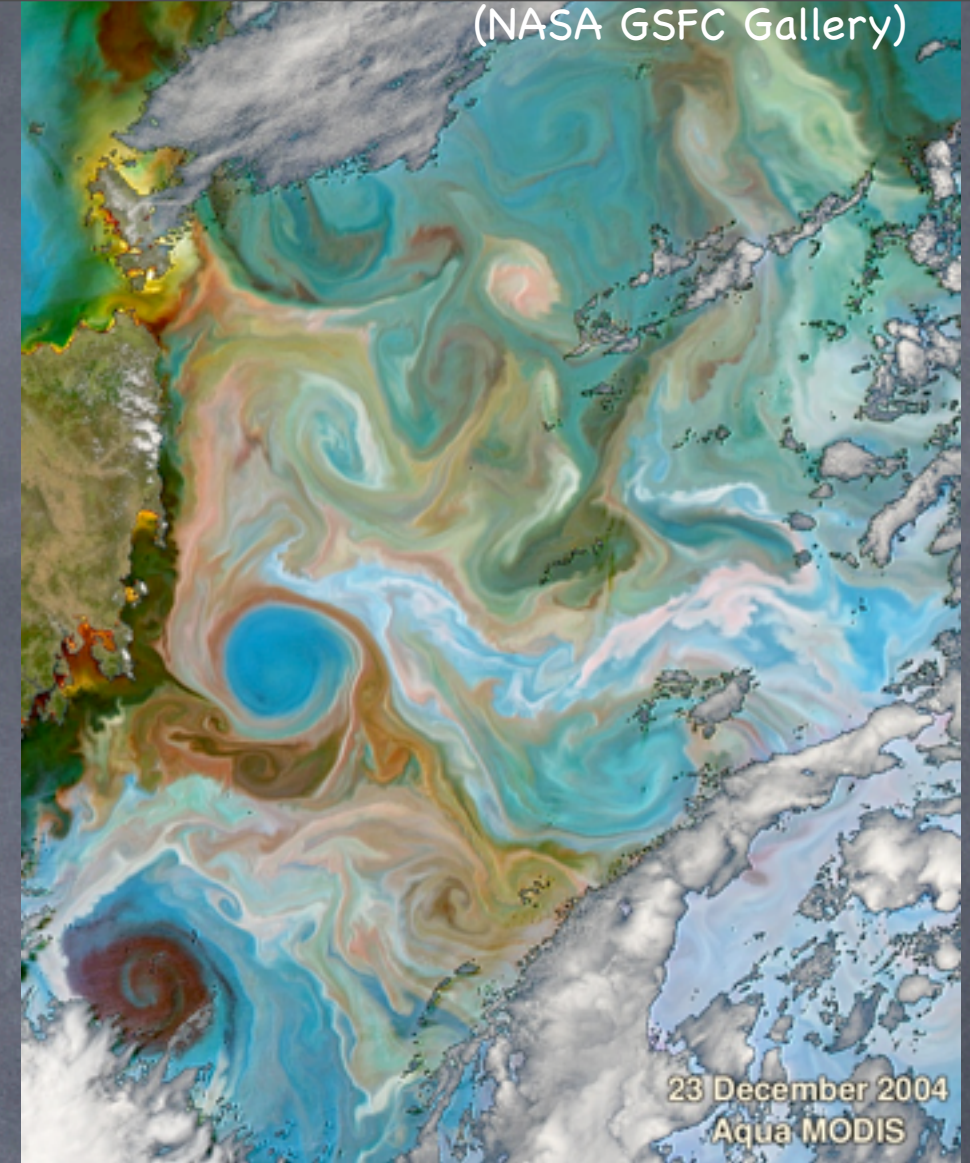




# The Character of the Finescale

(Capet et al., 2008)

(NASA GSFC Gallery)



100 m

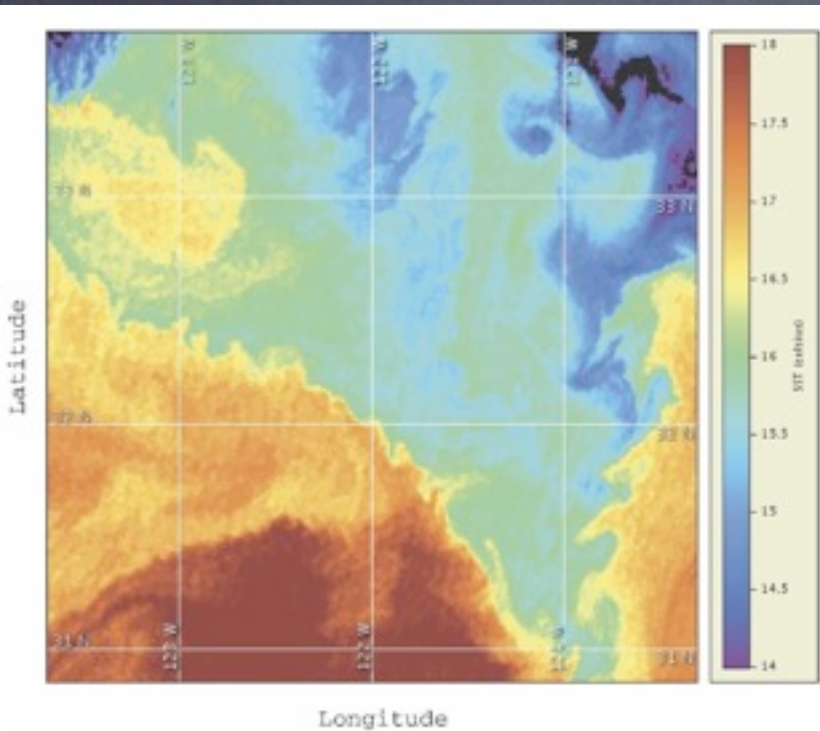


FIG. 16. Sea surface temperature measured at 1832 UTC 3 Jun 2006 off Point Conception in the California Current from CoastWatch (<http://coastwatch.pfeg.noaa.gov>). The fronts between recently upwelled water (i.e., 15°–16°C) and offshore water ( $\geq 17^\circ\text{C}$ ) show submesoscale instabilities with wavelengths around 30 km (right front) or 15 km (left front). Images for 1 day earlier and 4 days later show persistence of the instability events.

- 3d
- turbulent
- $Ro \gg 1$
- $Ri < 1$  to  $\ll 1$
- near-surface, bottom
- surface wave (Langmuir, breaking)
- internal waves/loss of balance/nonhydrostatic
- $< 100\text{m}$ , minutes-hrs.